Electronic, magnetic, and optical properties of relativistic Ruddlesden-Popper iridates

Peitao Liu

Faculty of Physics, Computational Materials Physics, University of Vienna, Vienna A-1090, Austria

Nov. 13th, 2019

Der Wissenschaftsfonds.

Outline:

- Motivation
- Electronic properties
  - Combined effect of SOC and U
  - Doping induced MIT
- Magnetic properties
  - Origin of different magnetic orderings in Sr_2IrO_4 and $Sr_3Ir_2O_7$
- Optical properties
- Summary

Why $Sr_{n+1}Ir_nO_{3n+1}$ (n=1, 2, and ∞)?

	3*d* (TMOs)	5*d* (TMOs)
d orbital	Localized	Spatially extended
Band width *W*	Small	Large
Hubbard *U*	Large (5~7 eV)	Small (1~3 eV)

Sr_2IrO_4

Ir^{4+} ($5d^5$)

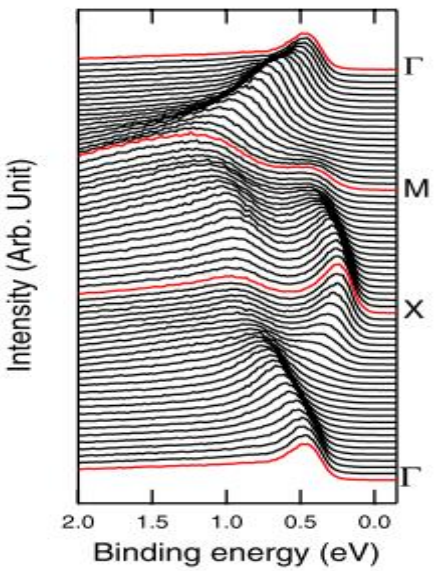

EDCs (ARPES)

Conventional Hubbard model :

U/W >> 1 Insulator

U/W <= 1 Metal

B. J. Kim *et al.*, PRL 101, 076402 (2008)

Why $Sr_{n+1}Ir_nO_{3n+1}$ (n=1, 2, and ∞)?

	3*d* (TMOs)	5*d* (TMOs)
d orbital	Localized	Spatially extended
Band width *W*	Small	Large
Hubbard *U*	Large (5~7 eV)	Small (1~3 eV)
SOC strength	Weak (~0.01-0.1 eV)	Strong (~0.1-1 eV)

Conventional Hubbard model :
U/W >> 1 Insulator
U/W <= 1 Metal

Sr_2IrO_4

Ir^{4+} ($5d^5$)

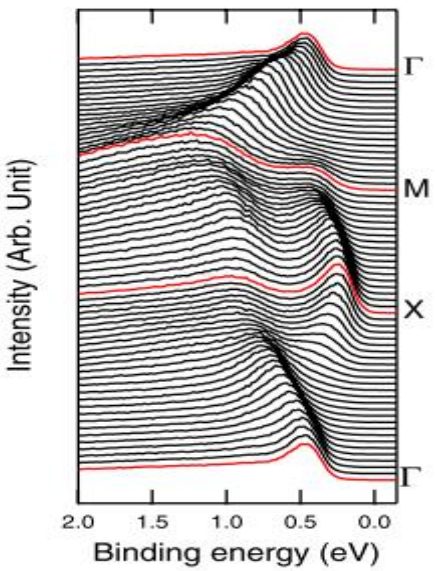

EDCs (ARPES)

B. J. Kim *et al.*, PRL 101, 076402 (2008)

Why $Sr_{n+1}Ir_nO_{3n+1}$ (n=1, 2, and ∞)?

- A novel spin-orbital J_{eff}=1/2 Mott state in Sr_2IrO_4

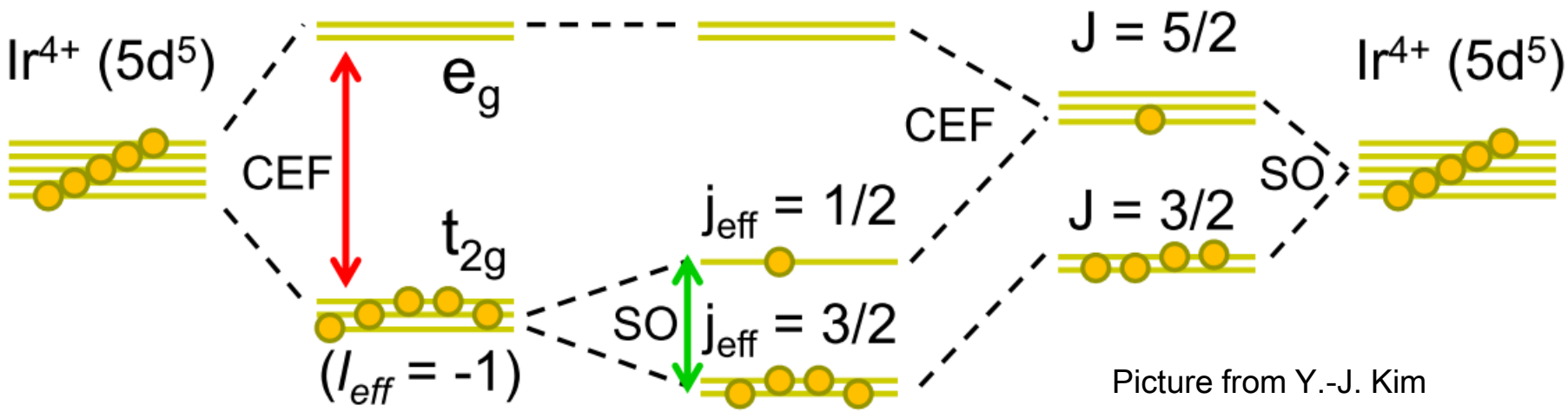

Picture from Y.-J. Kim

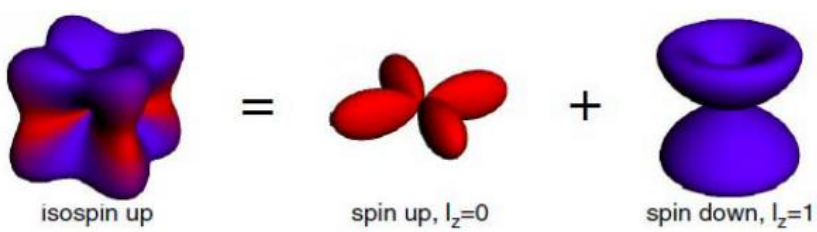

$$\frac{1}{\sqrt{3}}\left|xy,\uparrow\right\rangle+\frac{i}{\sqrt{3}}\left|xz,\downarrow\right\rangle+\frac{1}{\sqrt{3}}\left|yz,\downarrow\right\rangle$$

B. J. Kim *et al.,* PRL 101, 076402 (2008)
G. Jackeli et al, PRL 102, 017205 (2009)

Why $Sr_{n+1}Ir_nO_{3n+1}$ (n=1, 2, and ∞)?

- Possible superconductivity?

  - Similar crystal structure

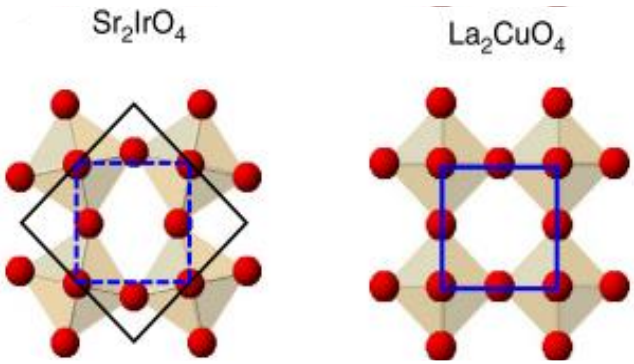

$I4_1/acd$ $I4/mmm$

  - Similar electronic configuration

La_2CuO_4 [$Cu^{2+}(3d^9)$, S=1/2]

Sr_2IrO_4 [$Ir^{4+}(5d^5)$, J_{eff}=1/2]

  - Theoretically possible by electron doping

    PRL 106, 136402 (2011)
    PRL 110, 027002 (2013)

  - Experimentally not observed yet

    Science 345,187(2014)
    PRL 115, 176402 (2015)
    Nat. Phys. 12, 37 (2016)

Why $Sr_{n+1}Ir_nO_{3n+1}$ (n=1, 2, and ∞)?

- Possible superconductivity?

  - Fermi arcs (electron doped Sr_2IrO_4)

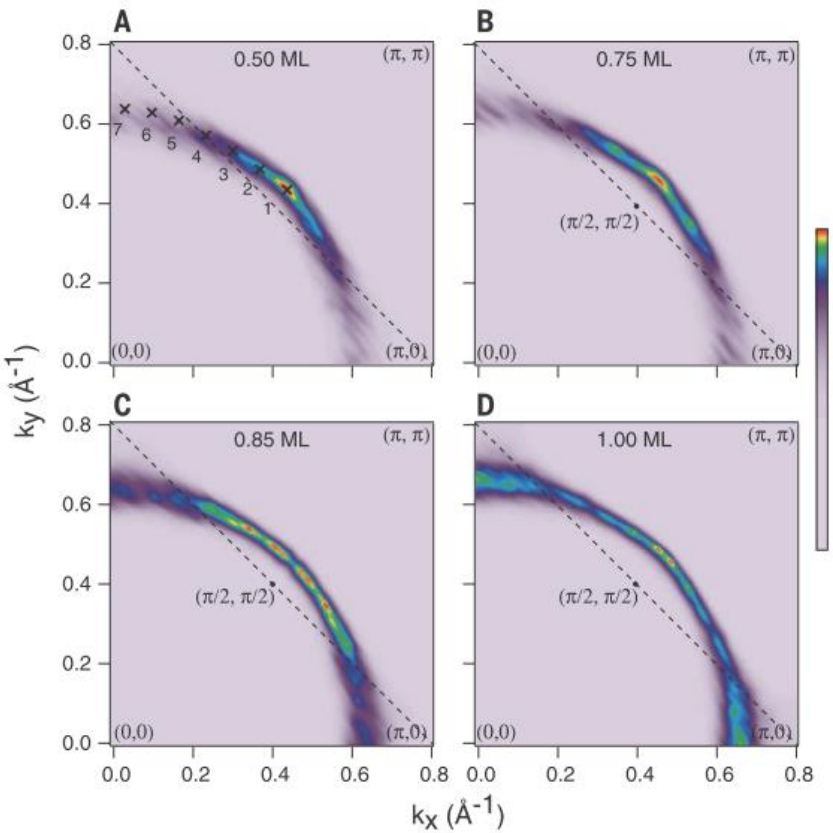

Y. K. Kim *et al.*, Science. 345, 187(2014)

  - Pseudogap (La doped Sr_2IrO_4)

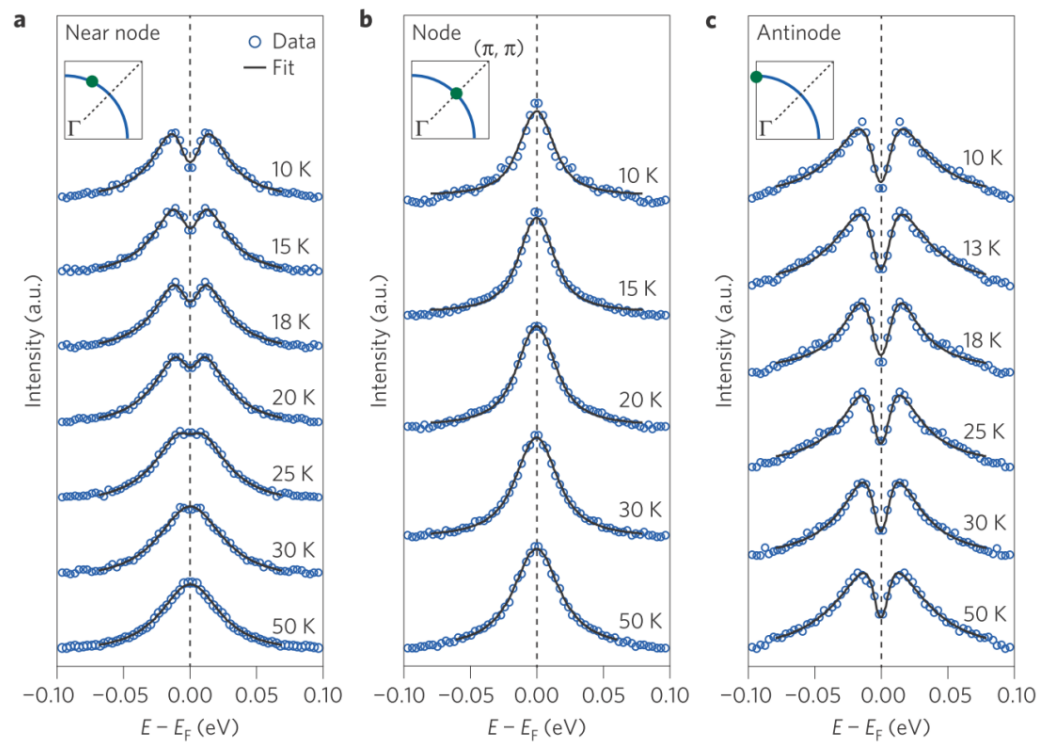

Y. K. Kim *et al.*, Nat. Phys. 12, 37(2016)

Why $Sr_{n+1}Ir_nO_{3n+1}$ (n=1, 2, and ∞)?

- Insulator-to-metal transition (IMT)

  - IMT is observed in La doped Sr_2IrO_4

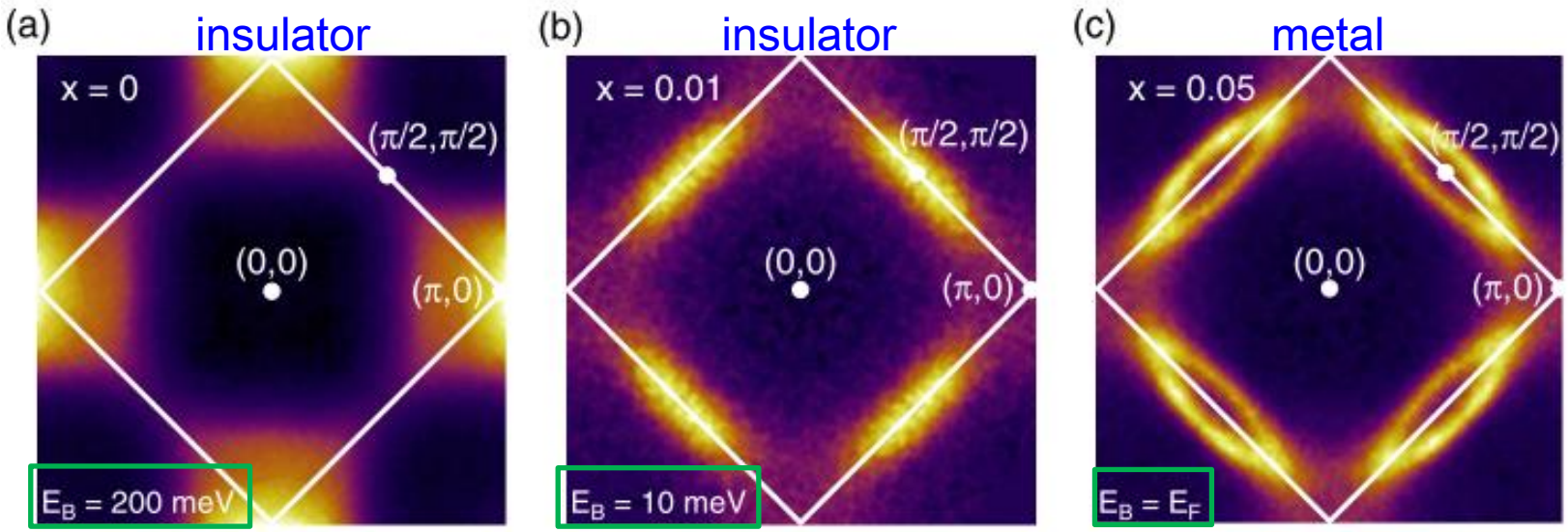

A. de la Torre *et al.*, PRL 115, 176402(2015)

Why $Sr_{n+1}Ir_nO_{3n+1}$ (n=1, 2, and ∞)?

- Insulator-to-metal transition (IMT)
  - IMT is observed in Rh doped Sr_2IrO_4

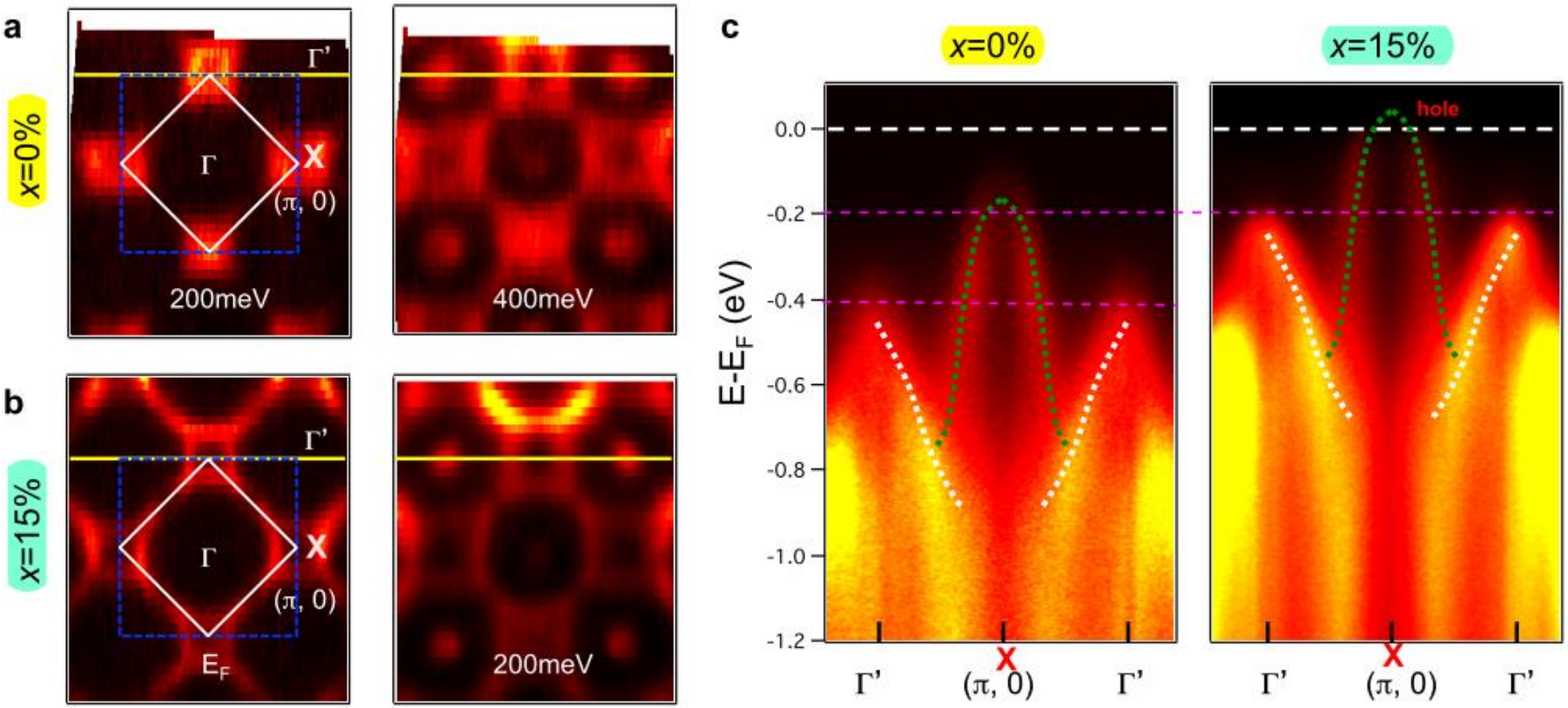

Y. Cao, et. al, arXiv:1406.4978 (2014)

Why $Sr_{n+1}Ir_nO_{3n+1}$ (n=1, 2, and ∞)?

- Unusual magnetic properties

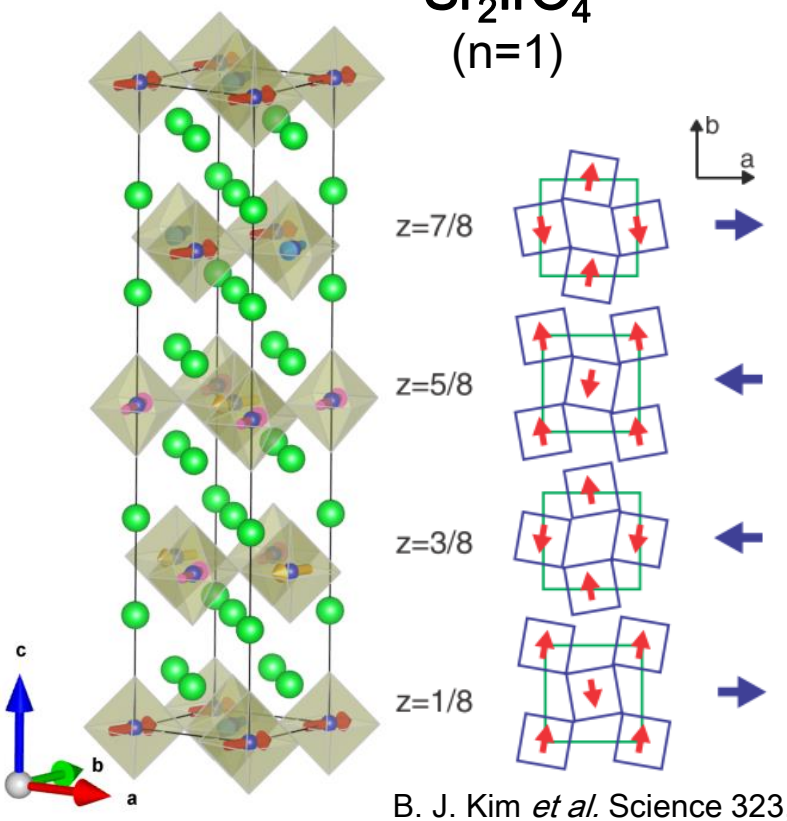

B. J. Kim *et al.* Science 323, 1329 (2009).

- In-plane canted anti-ferromagnetic ordering with a small net ferromagnetic moment.

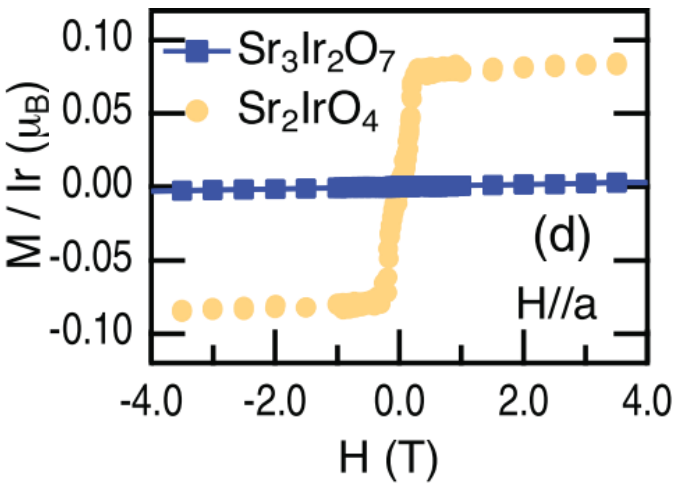

S. Fujiyama *et al.*, PRB 86, 174414 (2012)

Why $Sr_{n+1}Ir_nO_{3n+1}$ (n=1, 2, and ∞)?

- Unusual magnetic properties

$Sr_3Ir_2O_7$
(n=2)

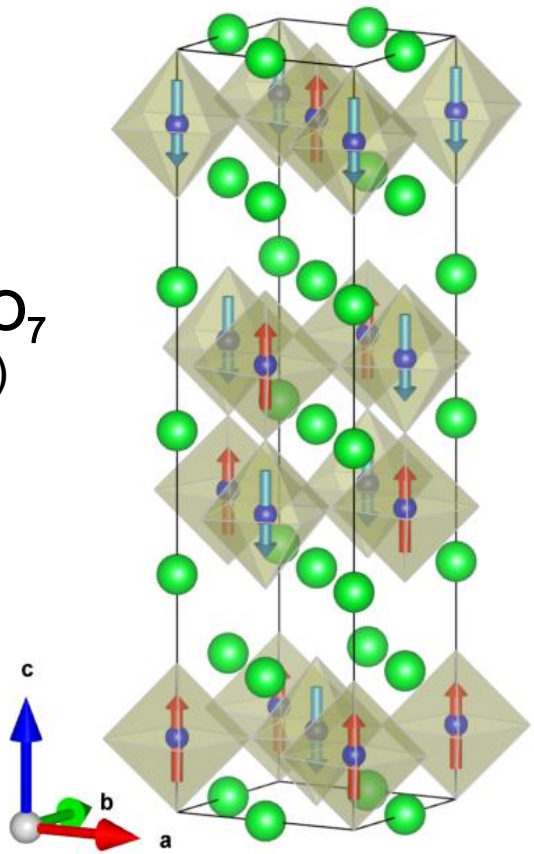

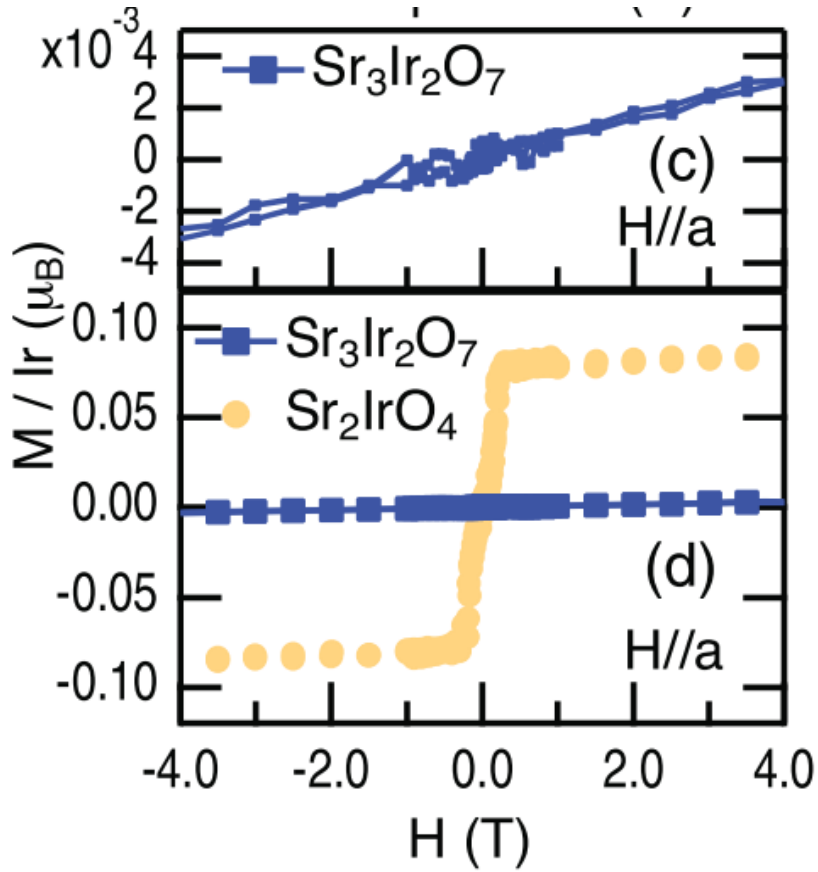

S. Fujiyama *et al.,* PRB 86, 174414 (2012)

- Out-of-plane collinear anti-ferromagnetic order, with negligible in-plane moment

Why $Sr_{n+1}Ir_nO_{3n+1}$ (n=1, 2, and ∞)?

- Unusual magnetic properties

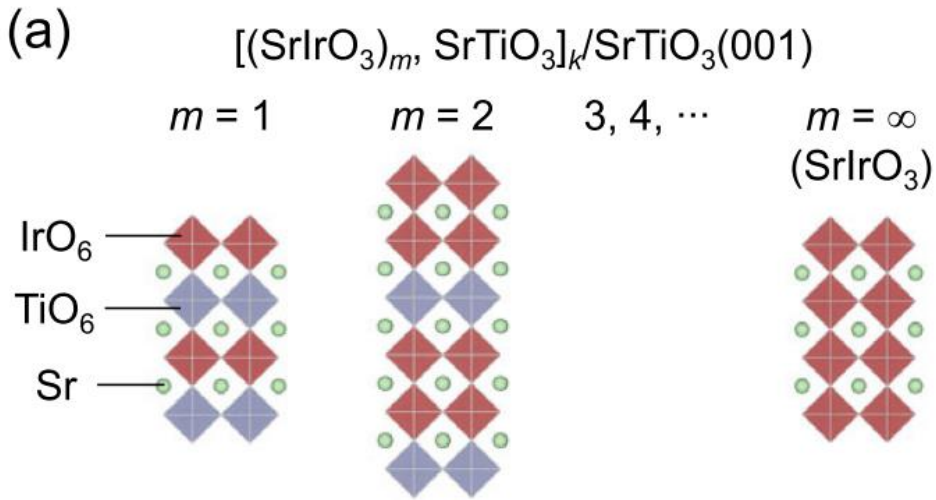

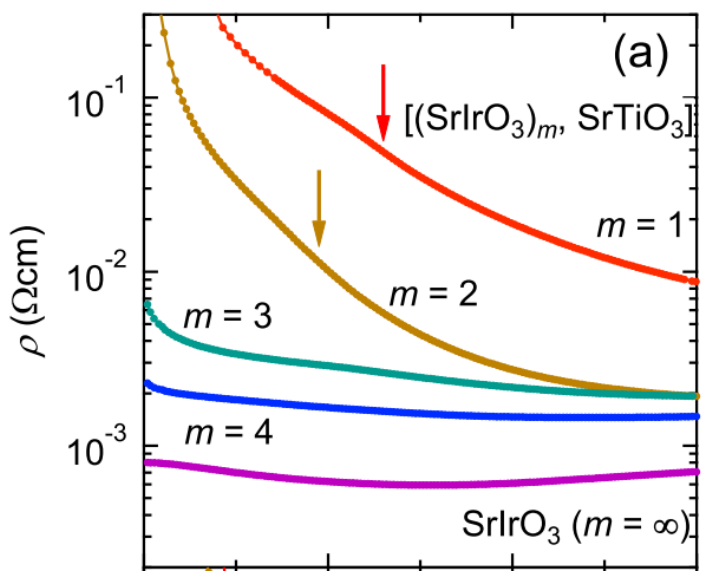

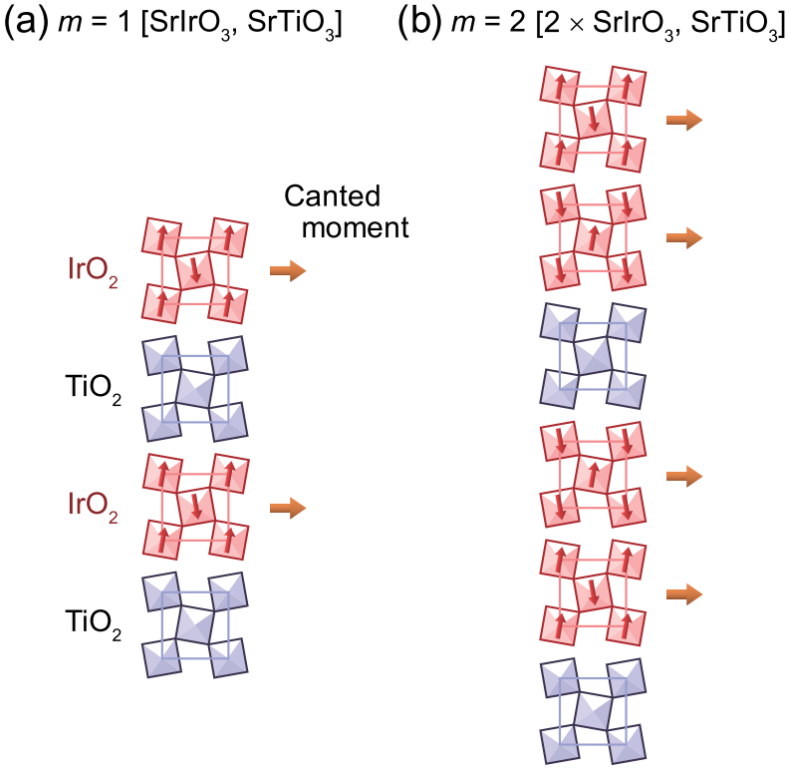

J. Matsuno, et al, PRL 114, 247209 (2015)

Why $Sr_{n+1}Ir_nO_{3n+1}$ (n=1, 2, and ∞)?

- Unusual magnetic properties

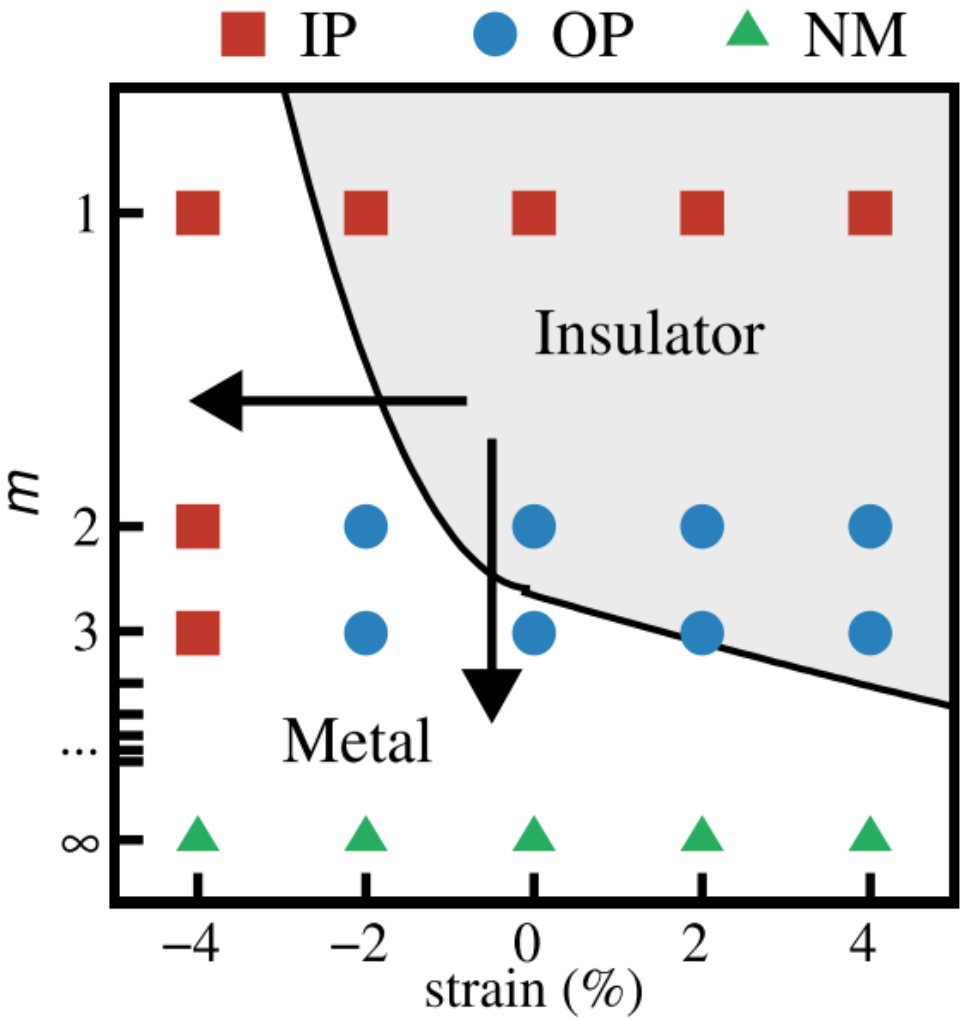

- $(SrIrO_3)_m/SrTiO_3$

B. Kim, P. Liu, et al, PRB 95, 115111 (2017)

Why $Sr_{n+1}Ir_nO_{3n+1}$ (n=1, 2, and ∞)?

- Unusual magnetic properties

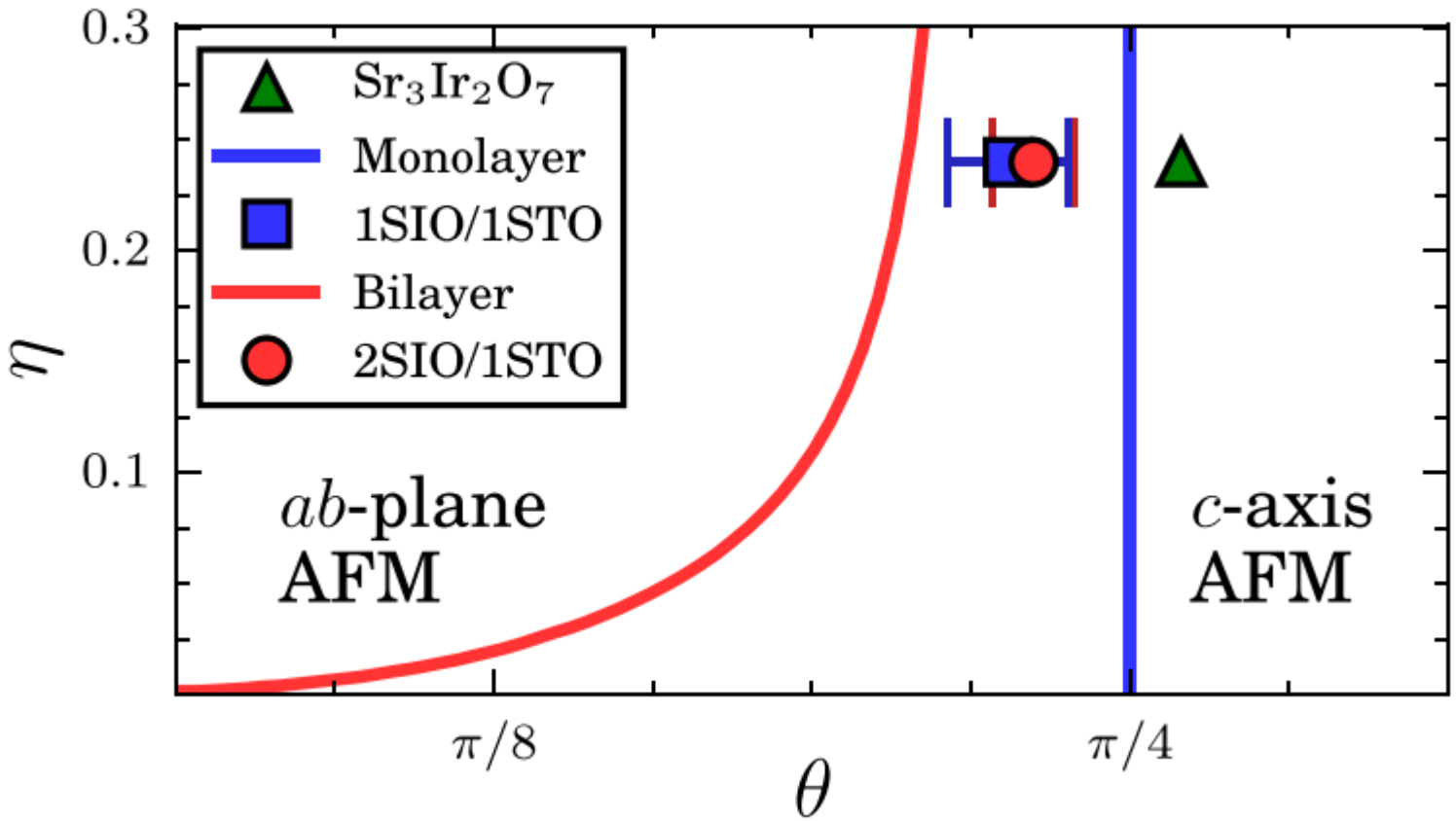

D. Meyers, et al, Scientific Reports 9, 4263 (2019)

Why $Sr_{n+1}Ir_nO_{3n+1}$ (n=1, 2, and ∞)?

➢ Dimensionality-controlled insulator-metal transition

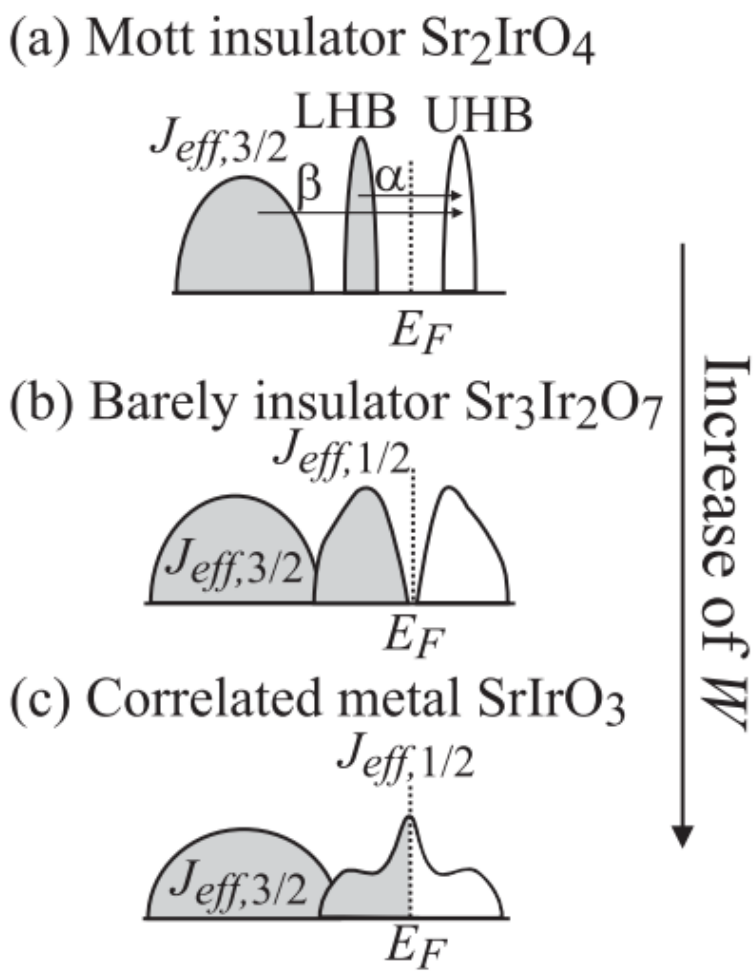

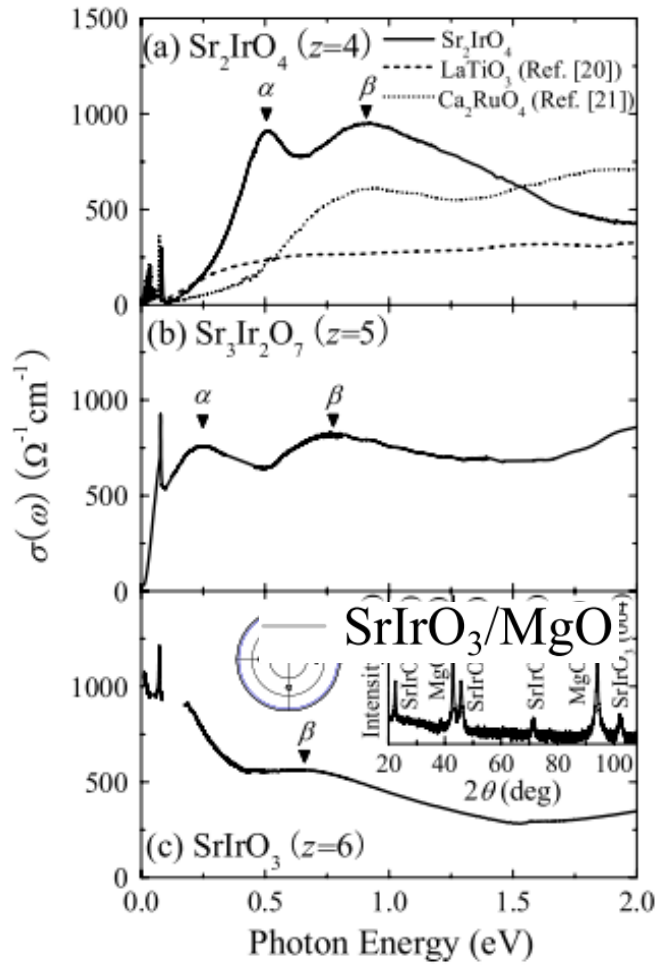

Single crystal

Single crystal

Thin film

S. J. Moon *et al.*, PRL 101, 226402 (2008).

Why $Sr_{n+1}Ir_nO_{3n+1}$ (n=1, 2, and ∞)?

$SrIrO_3$ polycrystalline sample

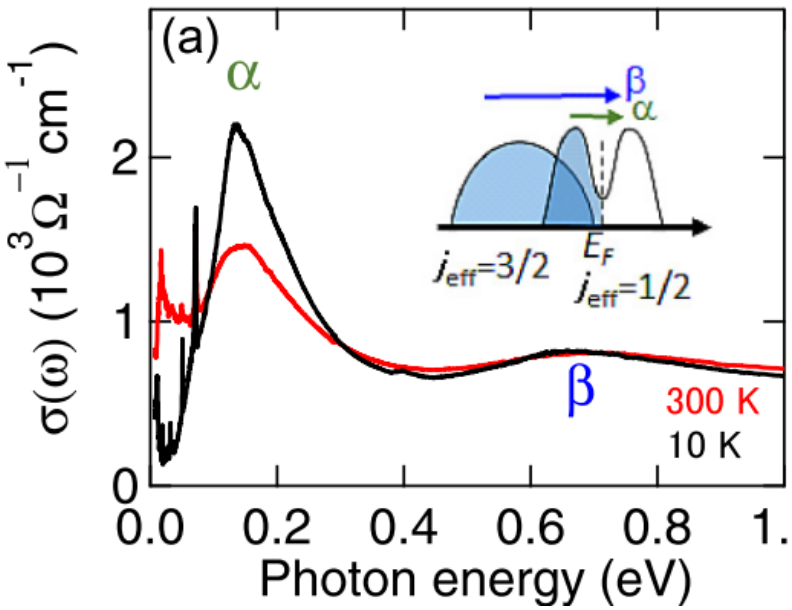

J. Fujioka *et al.*, PRB 95, 121102 (2017).

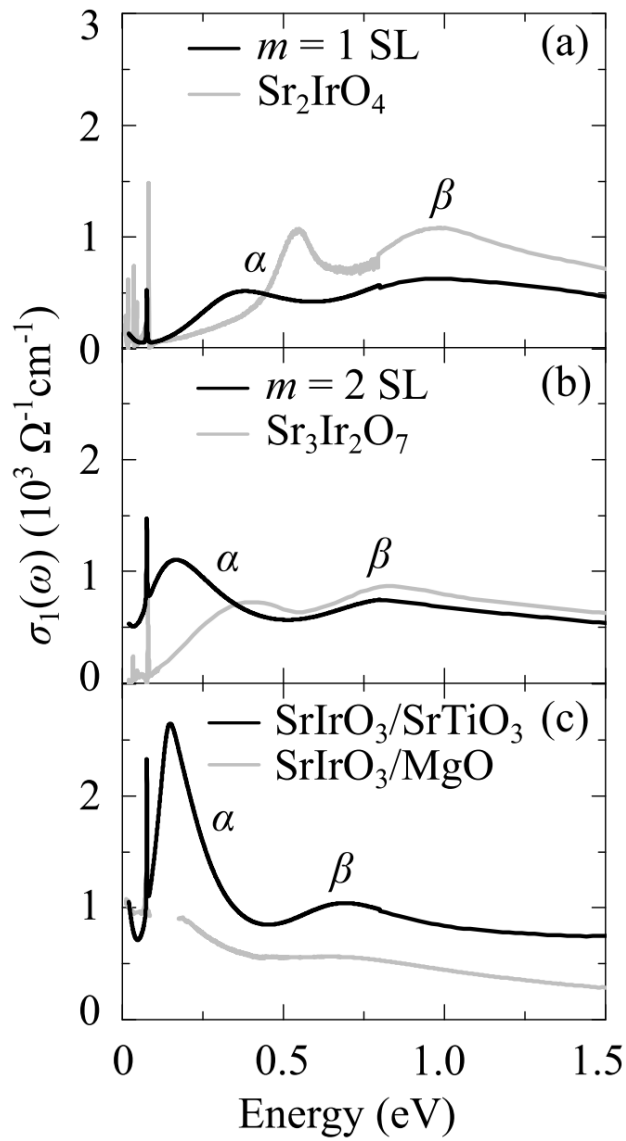

S. Y. Kim *et al.*, PRB 94, 245113 (2016).

Outline:

- Motivation
- Electronic properties
  - Combined effect of SOC and U
  - Doping induced MIT
- Magnetic properties
  - Origin of different magnetic orderings in Sr_2IrO_4 and $Sr_3Ir_2O_7$
- Optical properties
- Summary

Crystal structure

Sr_2IrO_4 (n=1)

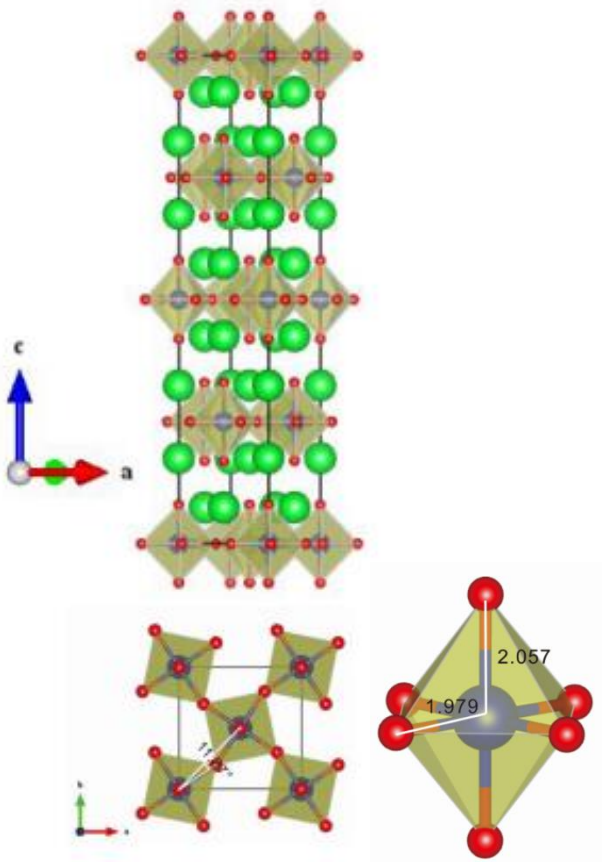

$I4_1/acd$ (142)

c/a =1.04

Rotation+distortion

One-layer quasi-2D

$Sr_3Ir_2O_7$ (n=2)

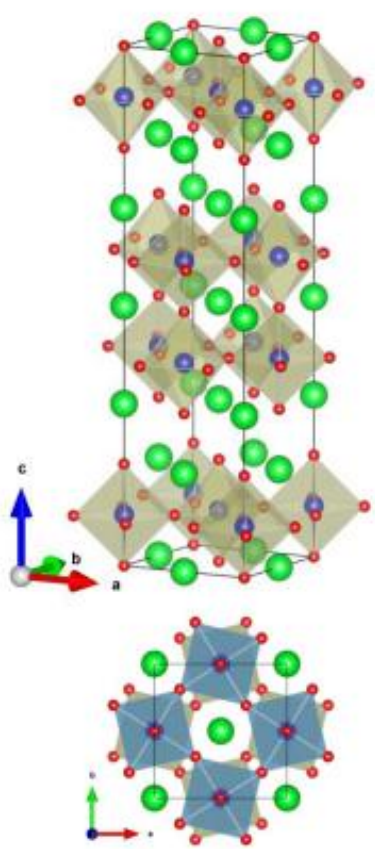

Ccce (68)

Staggered rotation+distortion

Bilayer quasi-2D

$SrIrO_3$ (n= ∞)

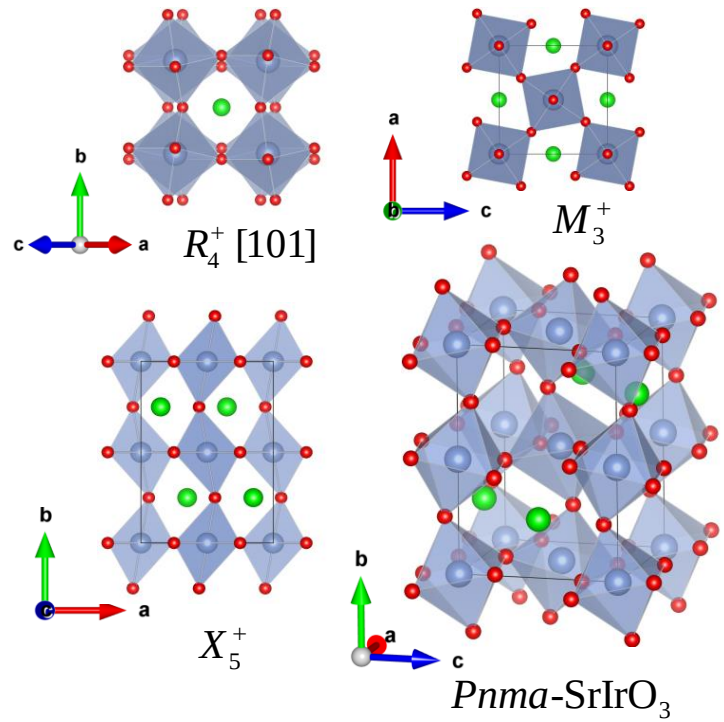

Pnma (62)

Rotation+tilt+distortion

Three-dimensional (3D)

Effects of U and SOC

Metal-insulator transition phase diagram

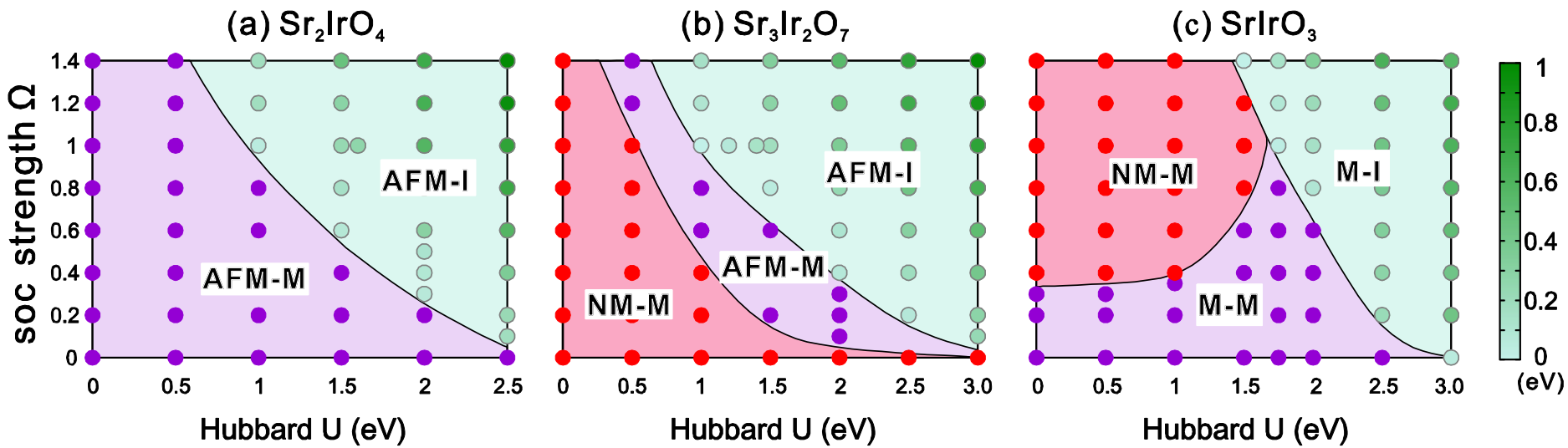

AFM-I - anti-ferromagnetic insulator AFM-M - anti-ferromagnetic metal
M-M - magnetic metal M-I - magnetic insulator NM-M - non-magnetic metal

- The stronger the SOC, the smaller is the critical interaction U_c required for a metal-insulator transition.
- Critical U_c to a metal-insulator transition : $Sr_2IrO_4 < Sr_3Ir_2O_7 < SrIrO_3$

Band structure evolution

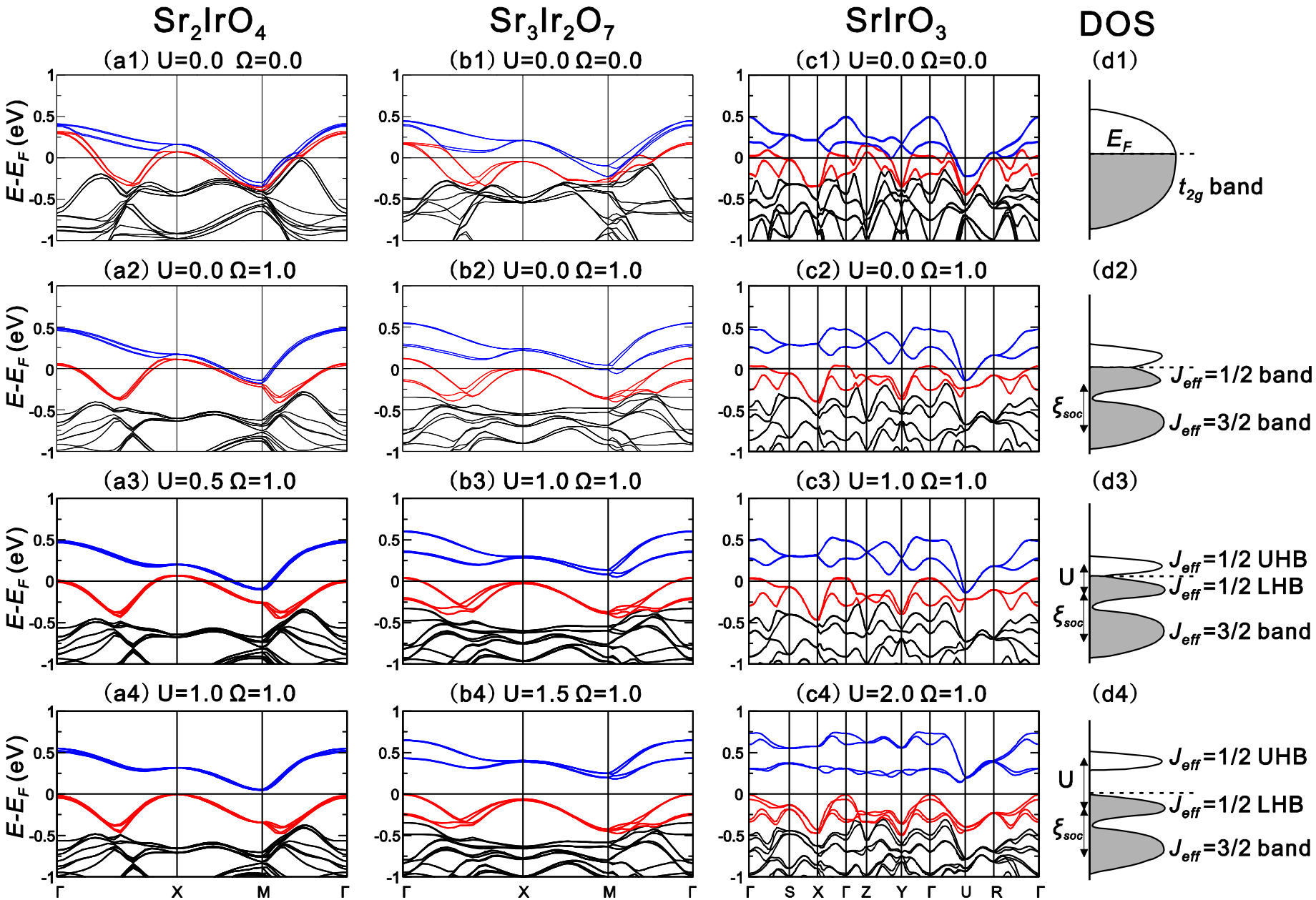

Calculating U based on cRPA

Aryasetiawan *et al.*, PRB**70**, 195104 (2004)

$$U_{mn}(\omega) = \langle \varphi_{m0}(\mathbf{r})\varphi_{m0}(\mathbf{r}) | \underline{W_r}(\mathbf{r},\mathbf{r}';\omega) | \varphi_{n0}(\mathbf{r}')\varphi_{n0}(\mathbf{r}') \rangle$$

$$W_r = \frac{v}{1 - \underline{P_r} v}$$

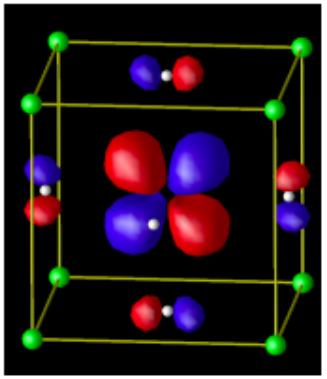

$$P(\mathbf{r},\mathbf{r}';\omega) = \sum_m^{\text{occ}} \sum_n^{\text{unocc}} \psi_m(\mathbf{r})\psi_n^*(\mathbf{r})\psi_m^*(\mathbf{r}')\psi_n(\mathbf{r}') \times \left\{ \frac{1}{\omega - \epsilon_n + \epsilon_m + i\delta} - \frac{1}{\omega + \epsilon_n - \epsilon_m - i\delta} \right\}$$

$$\sum_m^{\text{occ}} \sum_n^{\text{unocc}} = \sum_r^{\text{occ}} \sum_r^{\text{unocc}} + \sum_r^{\text{occ}} \sum_d^{\text{unocc}} + \sum_d^{\text{occ}} \sum_r^{\text{unocc}} + \cancel{\sum_d^{\text{occ}} \sum_d^{\text{unocc}}}$$

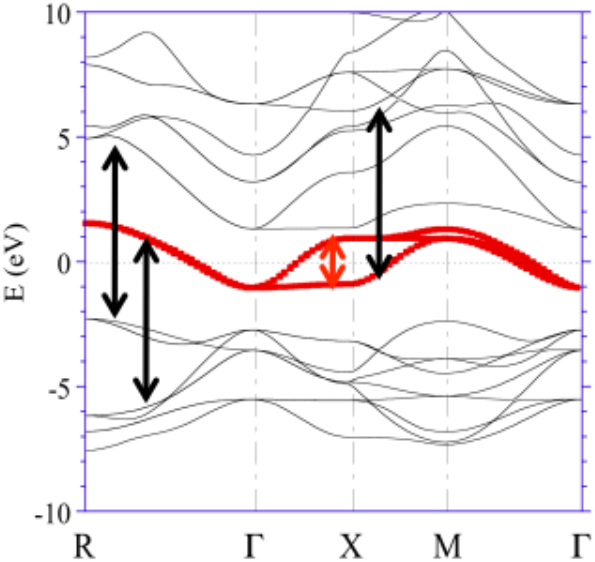

Picture from F. Aryasetiawan

Calculating U based on cRPA

- All the screening channels within t_{2g} subspace are removed
- U is calculated in the t_{2g} Wannier basis

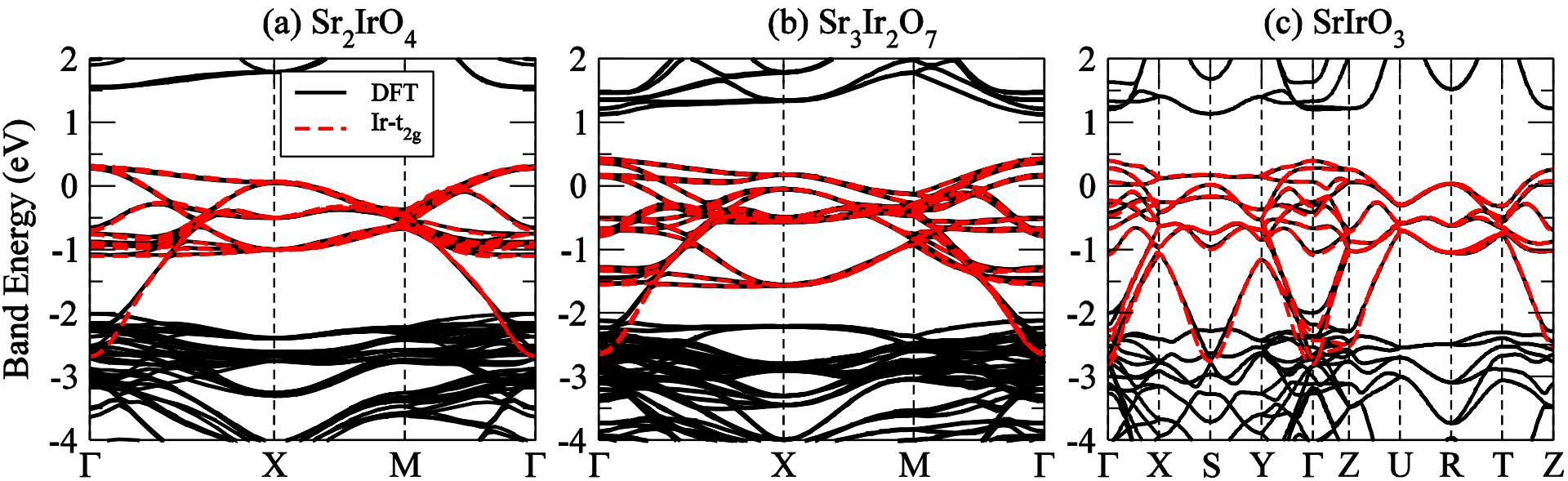

	U (eV)	J (eV)
Sr_2IrO_4	1.82	0.22
$Sr_3Ir_2O_7$	1.67	0.22
$SrIrO_3$	1.37	0.22

P. Liu *et al.*, PRM 2, 075003 (2018)

Band structure

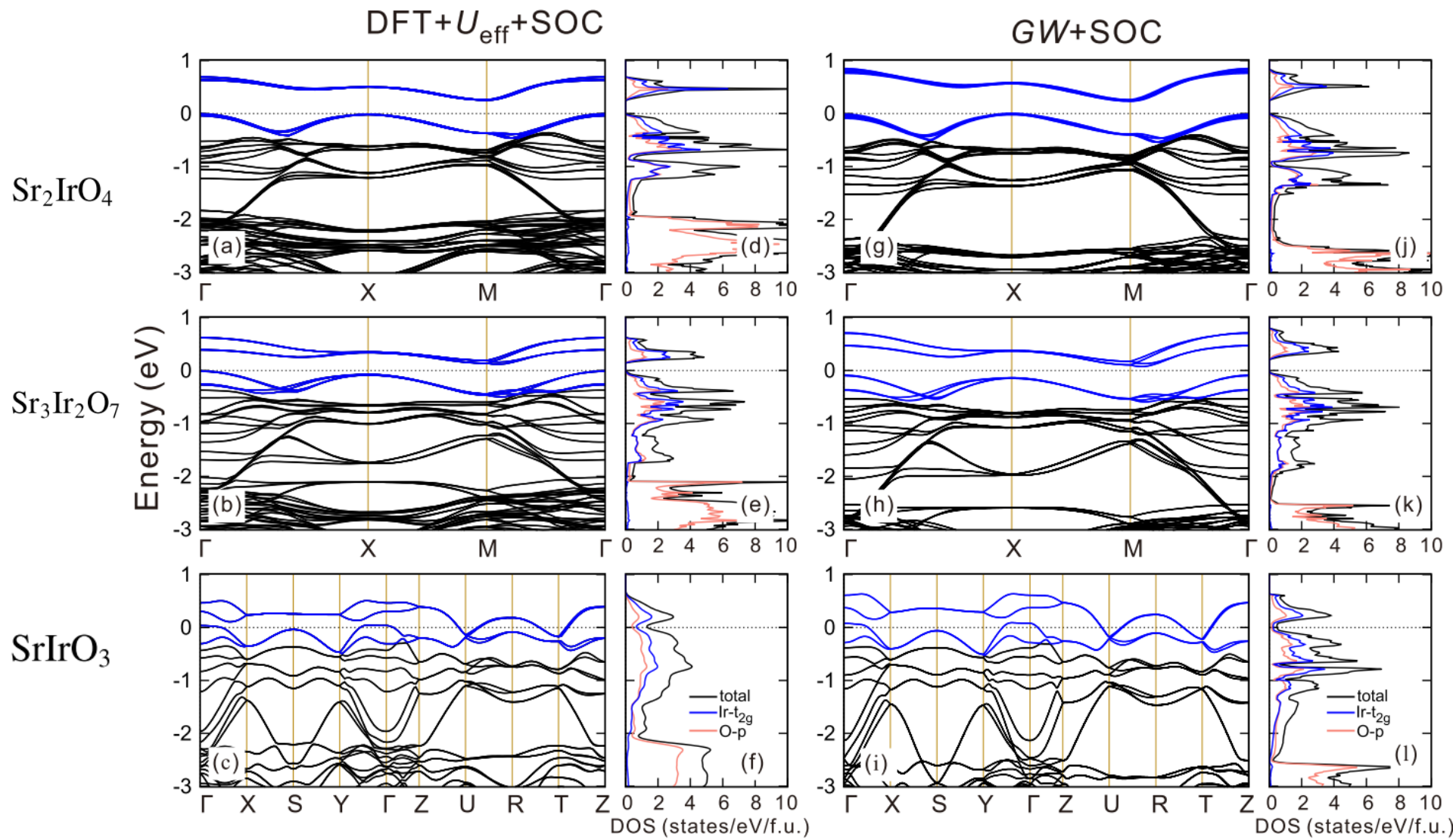

DFT+U_{eff} gap	0.23	0.14	metal
GW gap	0.25	0.16	metal
Expt. gap	0.30 [34]	0.13 [10]	metal [80,103]

P. Liu *et al.*, PRM 2, 075003 (2018)

Doping effects on the electronic structure in Sr_2IrO_4

➢ Supercell model

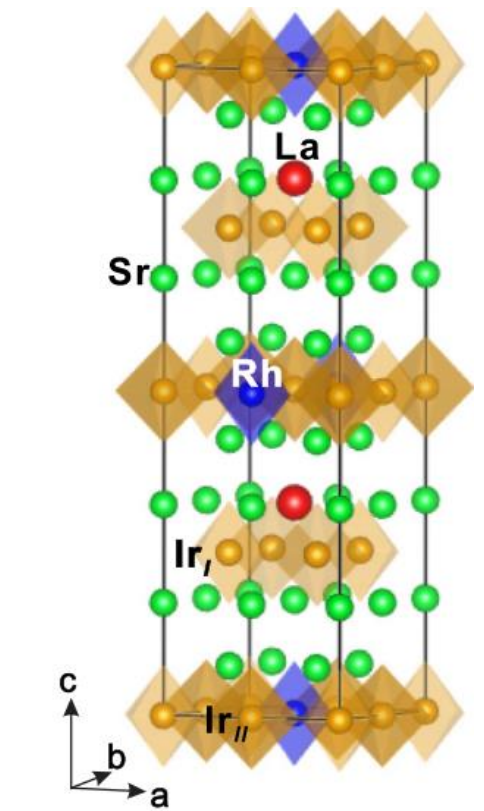

supercell $(\sqrt{2} \times \sqrt{2} \times 1)$

➢ Undoped Sr_2IrO_4

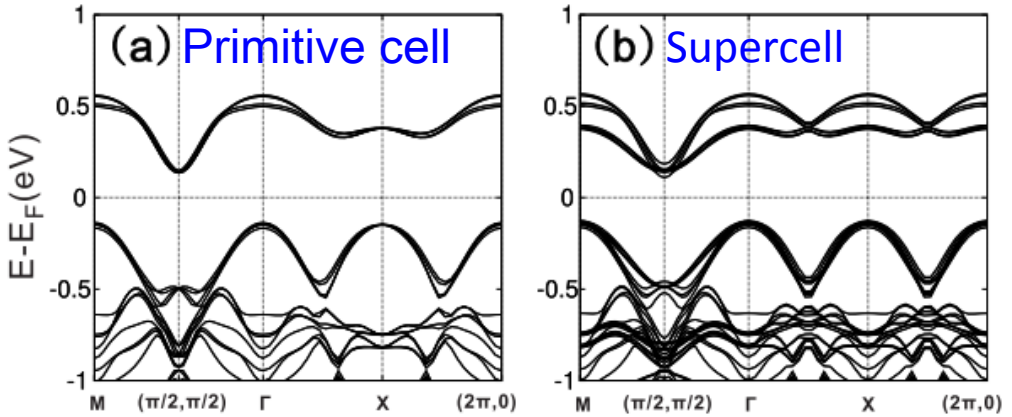

➢ Band unfolding

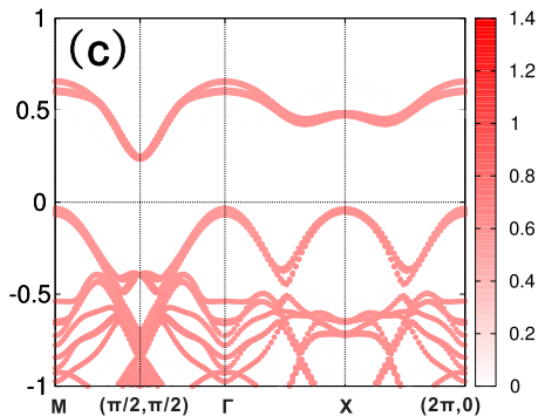

$$P_{\vec{K}m}(\vec{k}) = \sum_n |\langle \Psi_{\vec{K}m} | \psi_{\vec{k}n} \rangle|^2$$

P. Liu *et al.*, PRB 94, 195145 (2016)

Doping effects on the electronic structure in Sr_2IrO_4

- La doping

$$A(\vec{k},E) = \sum_m P_{\vec{K}m}(\vec{k})\delta(E_m - E)$$

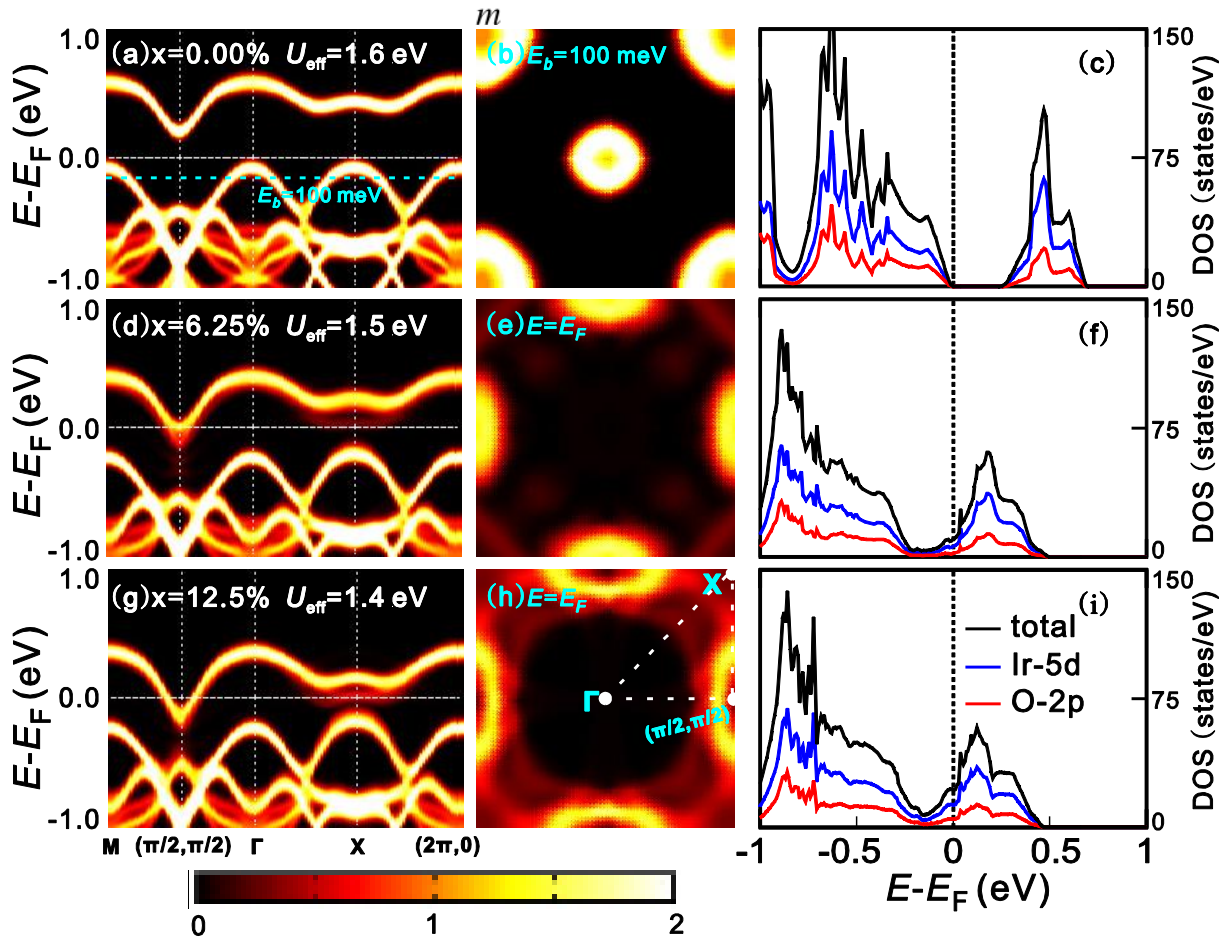

- Insulator to metal transition is found by La doping
- As La doping concentration increases, the upper Hubbard bands gradually shift down, leaving a electronic pocket first at $(\pi/2,\pi/2)$ and enhanced spectral function at X

P. Liu *et al.*, PRB 94, 195145 (2016)

Doping effects on the electronic structure in Sr_2IrO_4

➢ Rh doping

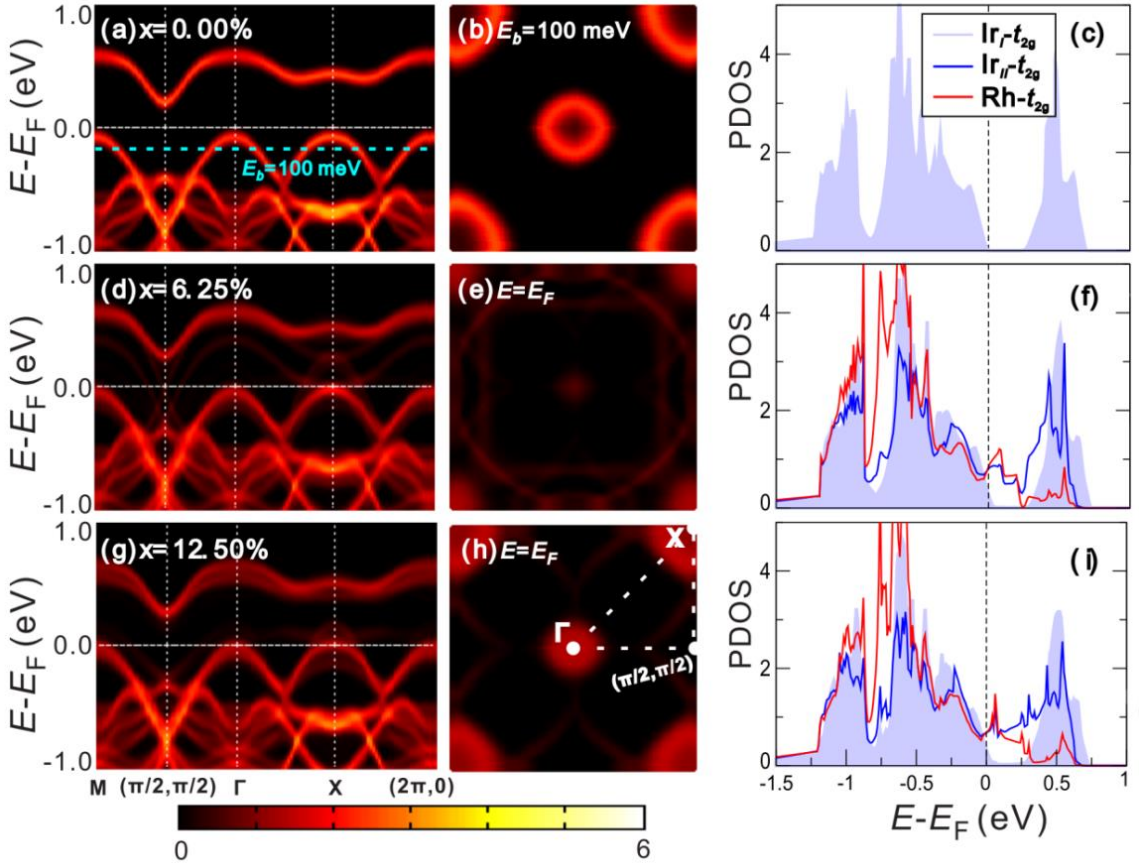

➢ Insulator to metal transition is found by Rh doping

➢ As Rh doping concentration increases, the lower Hubbard bands gradually shift up, leaving a hole pocket first at X and then at G

P. Liu *et al.*, PRB 94, 195145 (2016)

Doping effects on the electronic structure in Sr_2IrO_4

➢ Rh doping

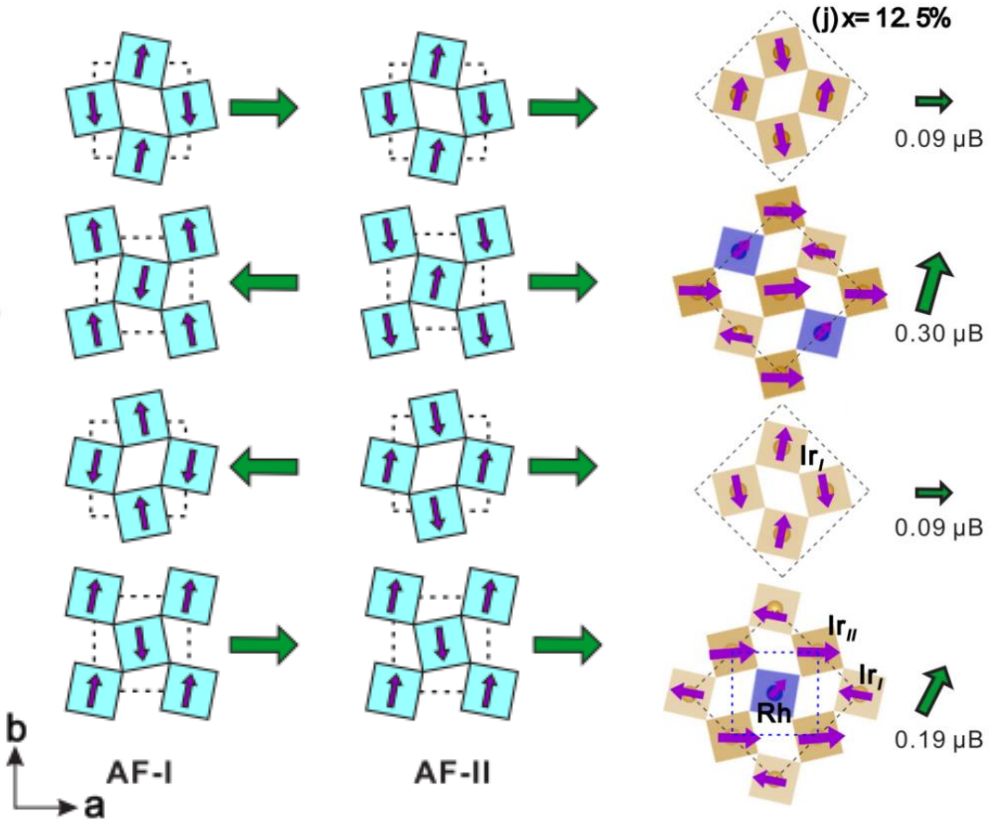

P. Liu *et al.,* PRB 94, 195145 (2016)

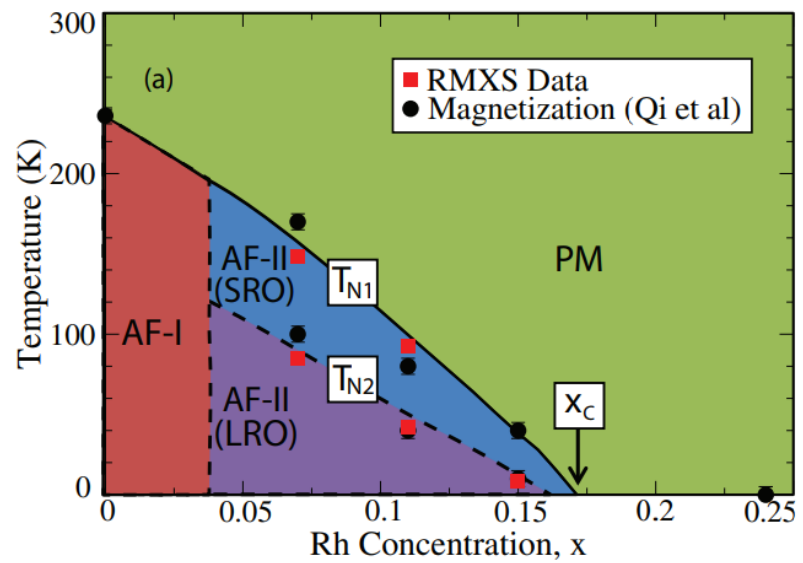

J. P. Clancy et al, PRB 89, 054409 (2014)

➢ Higher Rh doping leads to the magnetic phase transitions from AFM-I to AFM-II

Doping effects on the electronic structure in Sr_2IrO_4

➢ Rh doping

Electron charge density difference

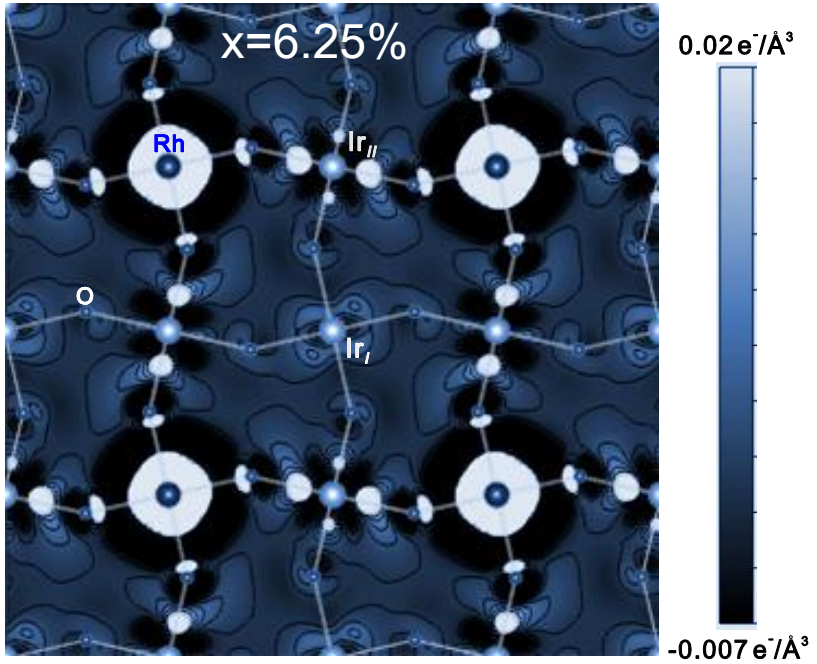

P. Liu *et al.,* PRB 94, 195145 (2016)

X-ray absorption near edge structure measurements

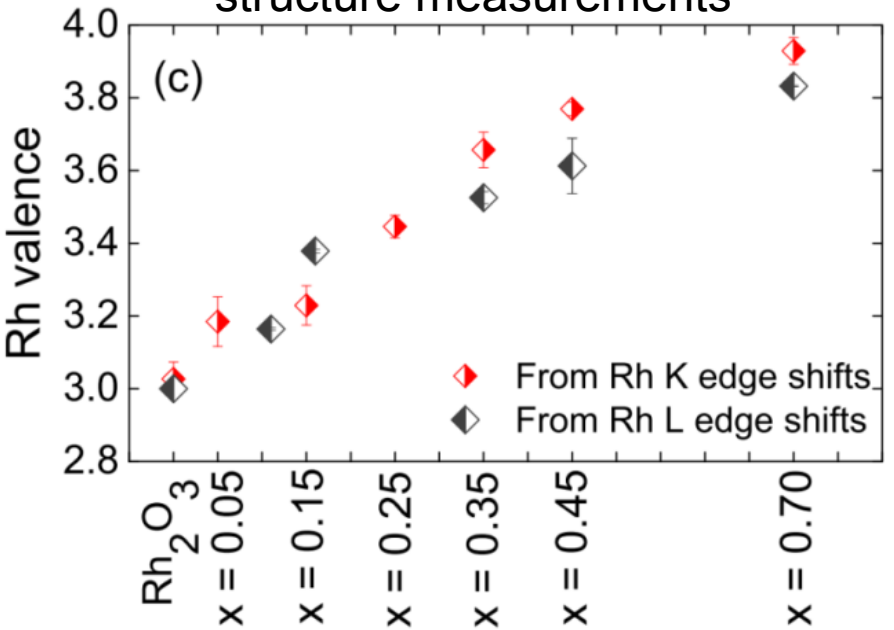

S. Chikara *et al.,* PRB 95, 060407(R) (2017)

- ➢ The effect of Rh doping is local, with negligible effect on the 2NN Ir.
- ➢ Hole transfer from Rh to NN Ir, leading to $Rh^{3.3+}$

Outline:

- Motivation
- Electronic properties
  - Combined effect of SOC and U
  - Doping induced MIT
- Magnetic properties
  - Origin of different magnetic orderings in Sr_2IrO_4 and $Sr_3Ir_2O_7$
- Optical properties
- Summary

Origin of the canted magnetism in Sr_2IrO_4

$$\mathcal{H} = \sum_{i<j} J\vec{S}_i \cdot \vec{S}_j + \sum_{i<j} J_z S_i^z S_j^z + \sum_{i<j} \vec{D} \cdot [\vec{S}_i \times \vec{S}_j] \quad (1)$$

$$\Delta E = 16JS^2\cos(2\theta) + 8K\cos(4\theta) + 16D_zS^2\sin(2\theta) \quad (2)$$

Constraining magnetic moments approach

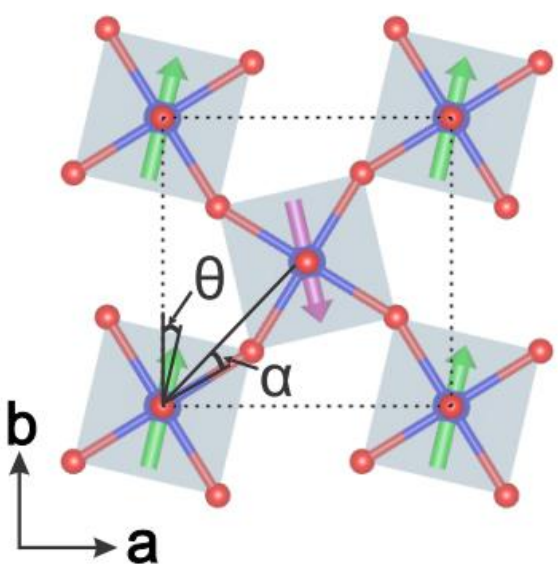

$$E = E_0 + \sum_i \lambda[\mathbf{M}_i - \mathbf{M}_i^0(\mathbf{M}_i^0 \cdot \mathbf{M}_i)]^2 \quad (3)$$

E_0 is the usual DFT energy without any constraint

$\mathbf{M}_i^0$ is a unit vector along the desired direction of the magnetic moment at site i

$\mathbf{M}_i$ is the integrated magnetic moment inside the Wigner-Seitz cell around atom i

λ controls the penalty energy contribution which becomes vanishingly small by increasing λ

P. Liu *et al.*, PRB.92.054428 (2015)

Origin of the canted magnetism in Sr_2IrO_4

$$\Delta E = 16JS^2\cos(2\theta) + 8K\cos(4\theta) + 16D_zS^2\sin(2\theta)$$

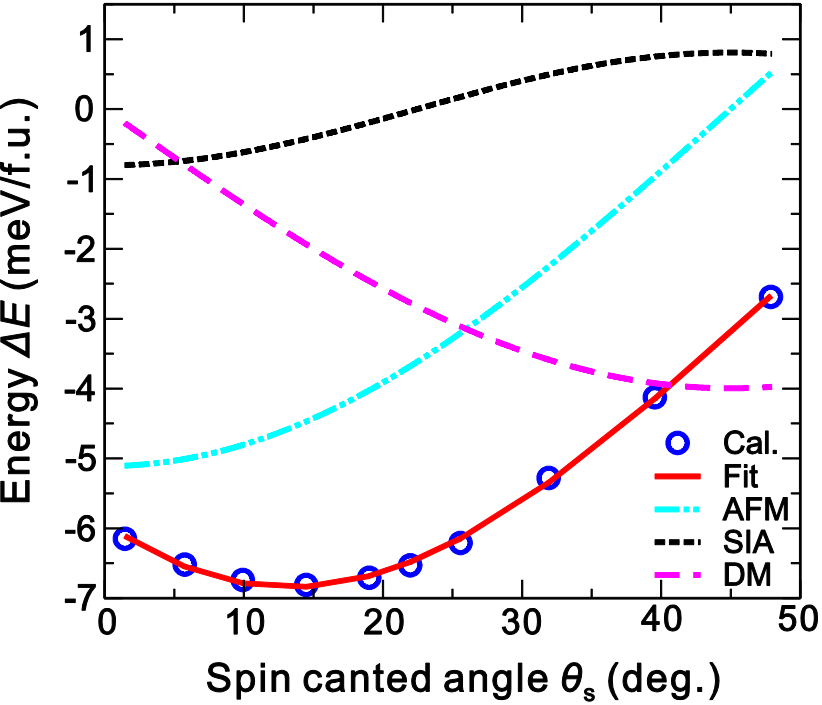

	JS^2	K	D_zS^2
This work	-0.32	-0.10	0.25
Literature	-(0.33~0.56)[a]	—	0.38[b]

[a] J. Kim, PRL (2012). B. H. Kim, PRL (2012). V. M. Katukuri, PRB (2012). G. Jackeli, PRL (2009).
[b] B. H. Kim, PRL (2012).

P. Liu *et al.*, PRB.92.054428 (2015)

Origin of the unusual magnetism in Sr_2IrO_4

Effects of tetragonal distortion and octahedral rotation

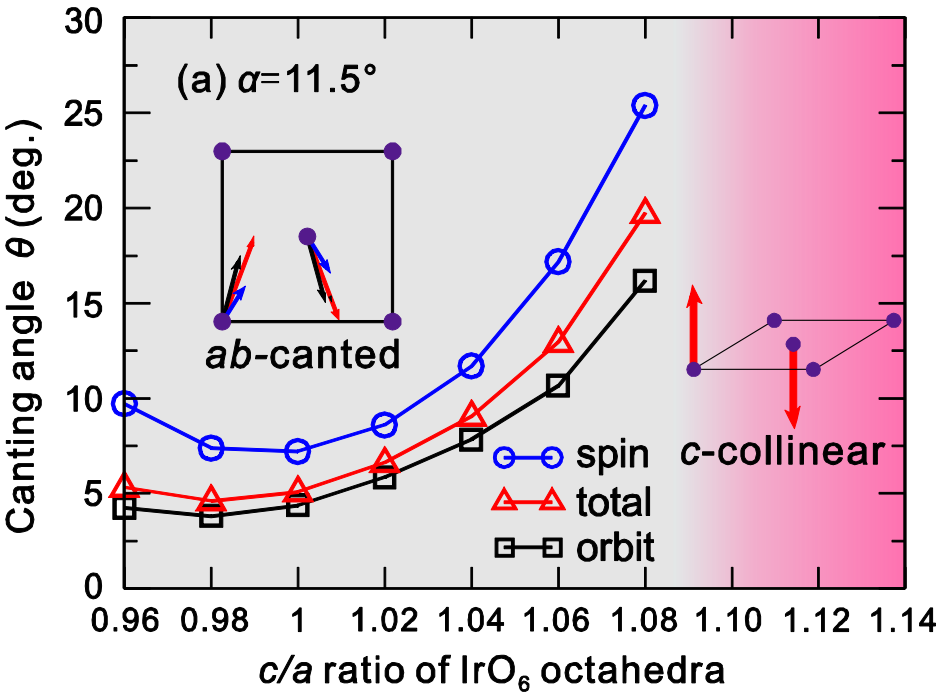

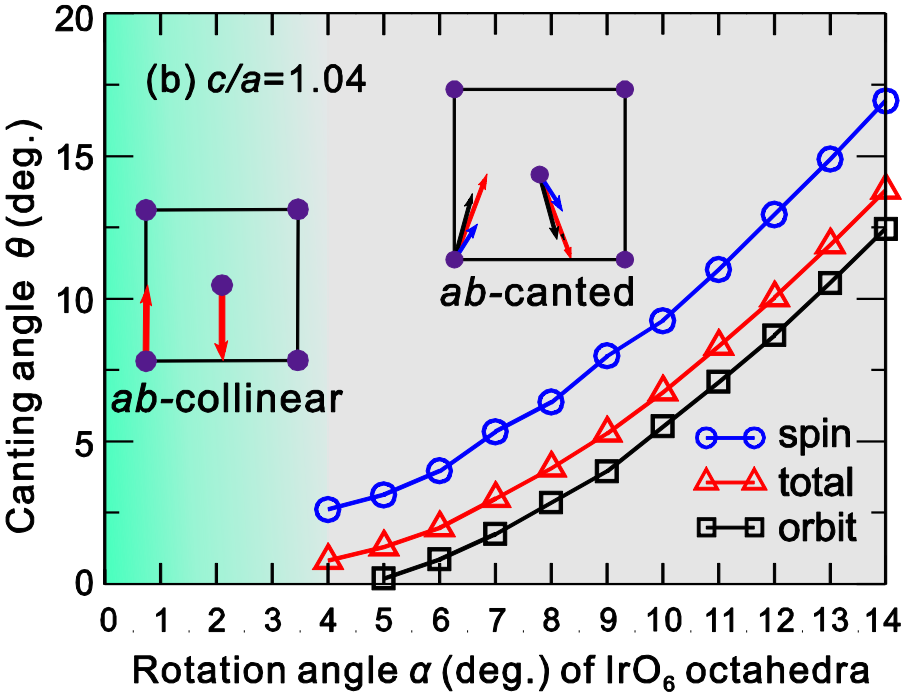

- As *c/a* increases to a threshold, spin-flop transition occurs
- As *α* decreases to a critical value, canted FM moment disappears

P. Liu *et al.*, PRB.92.054428 (2015)

Origin of the unusual magnetism in Sr_2IrO_4

Ab initio magnetic phase diagram in the *c/a*-*α* space

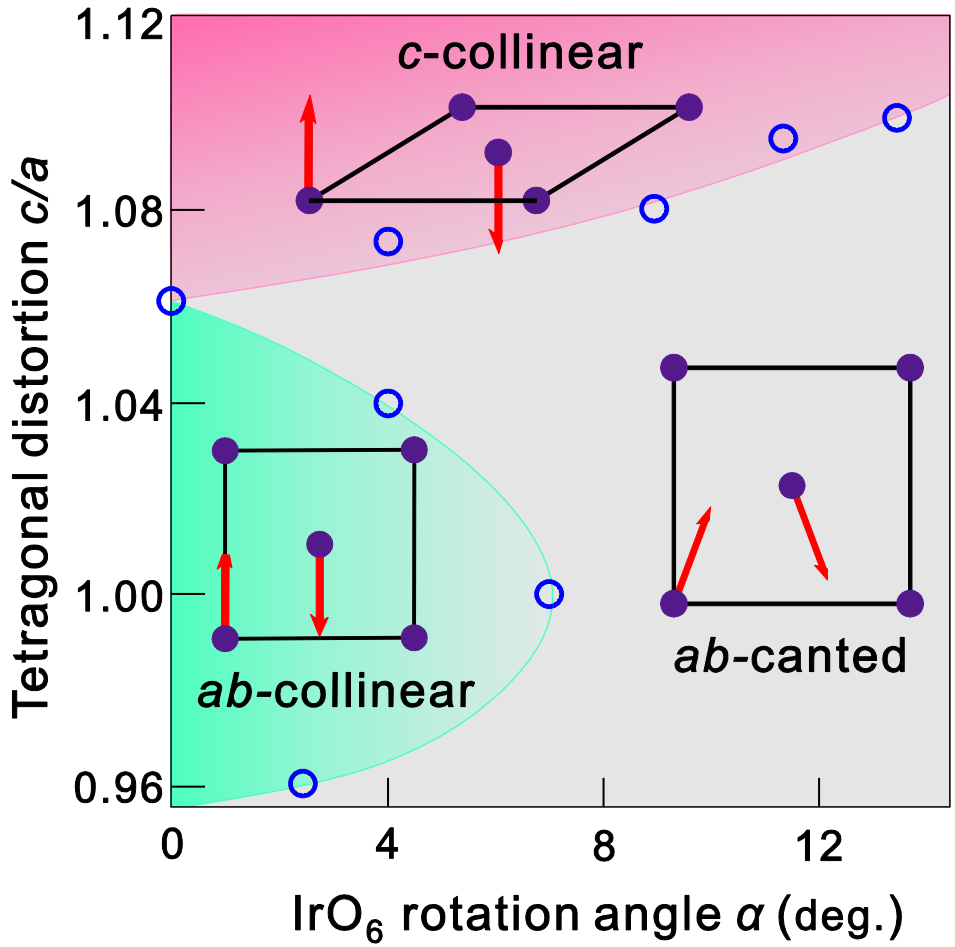

P. Liu *et al.*, PRB.92.054428 (2015)

Origin of the unusual magnetism in Sr_2IrO_4

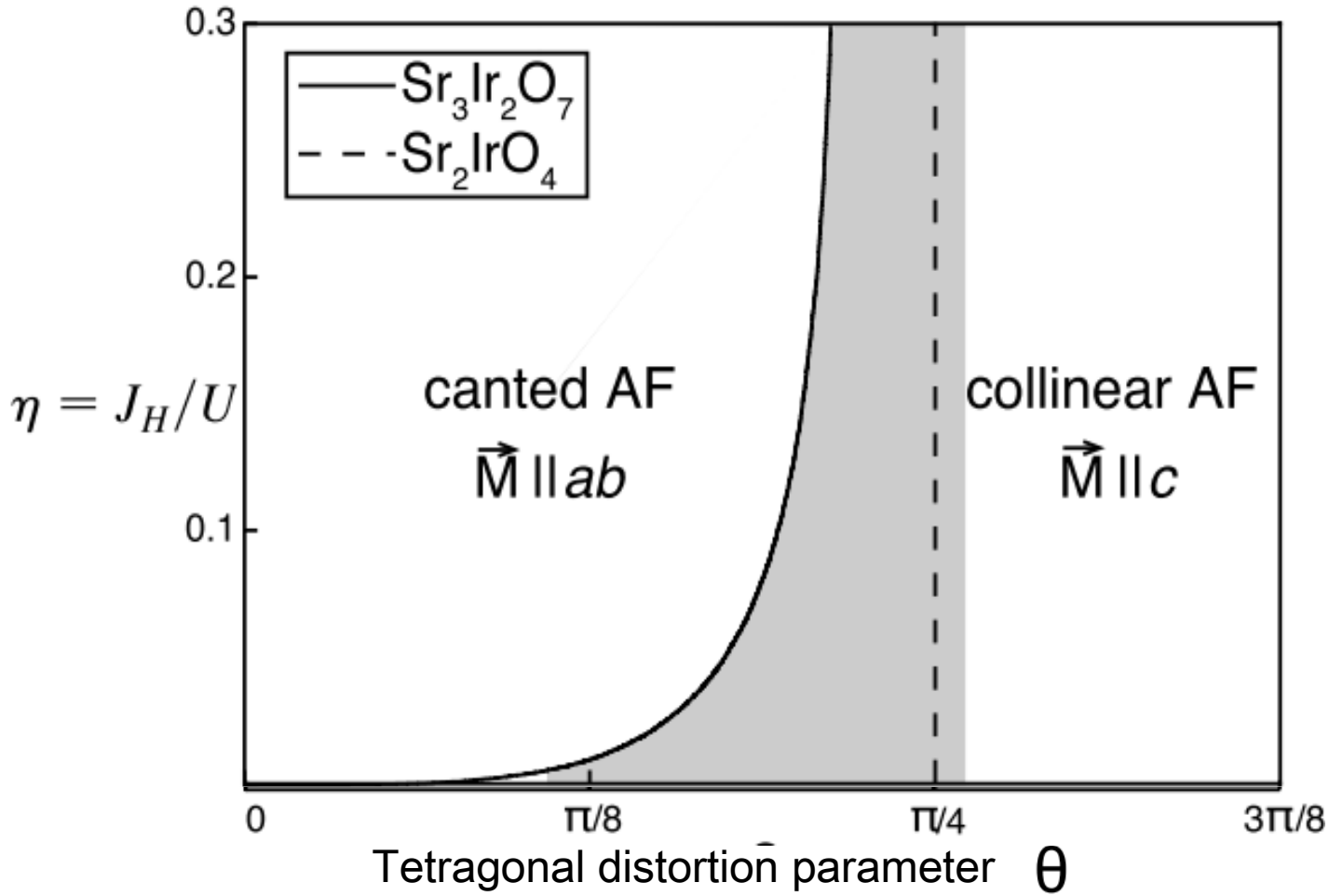

J. W. Kim *et al.,* PRL 109, 037204 (2012)

Possible reason for c-collinear AFM in $Sr_3Ir_2O_7$

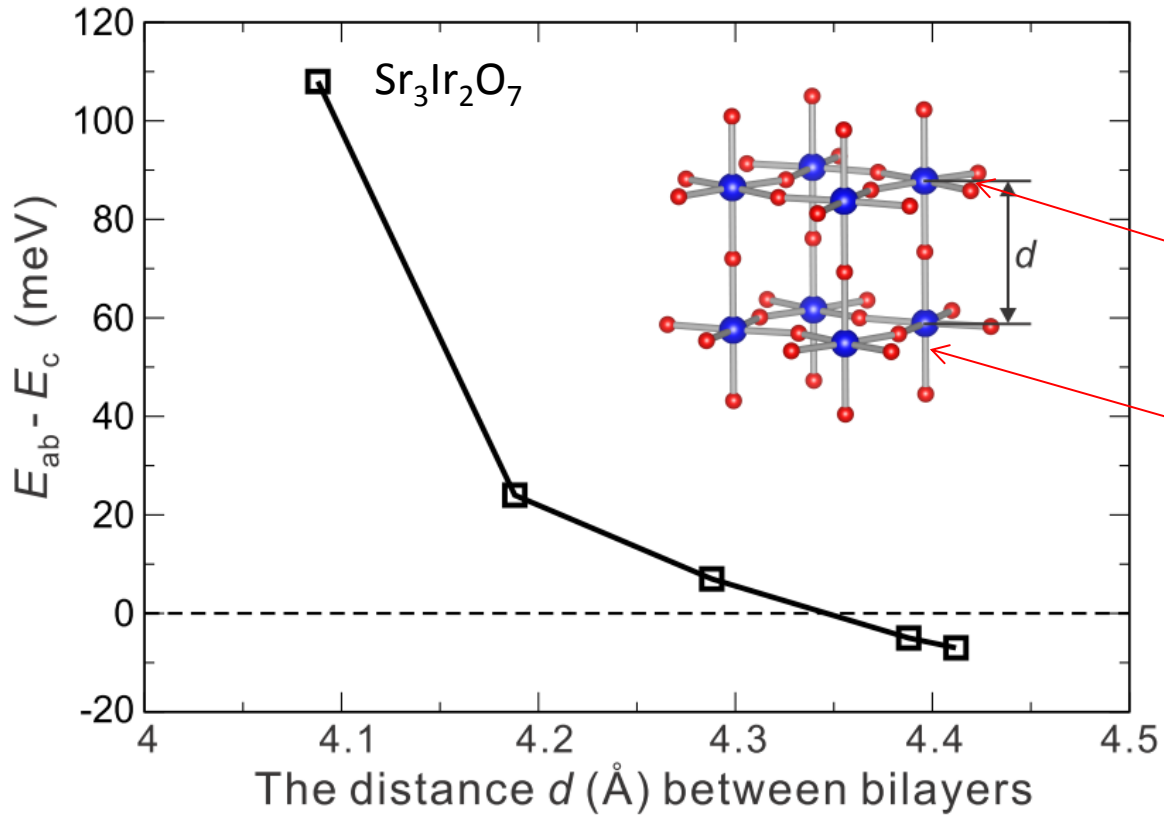

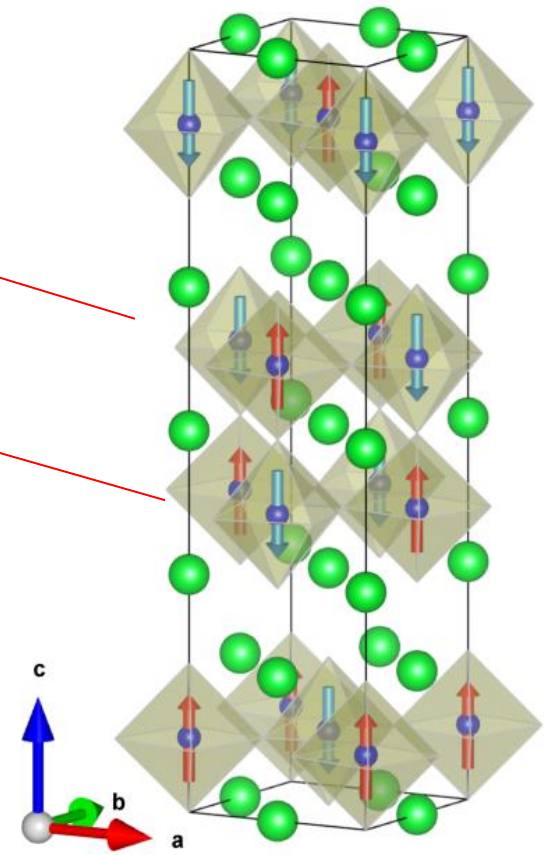

- The c-collinear AFM phase is favorable as the interlayer's distance <4.35 A.
- As the distance increases further, the ab-canted AFM becomes energetically stable phase.

Possible reason for c-collinear AFM in $Sr_3Ir_2O_7$

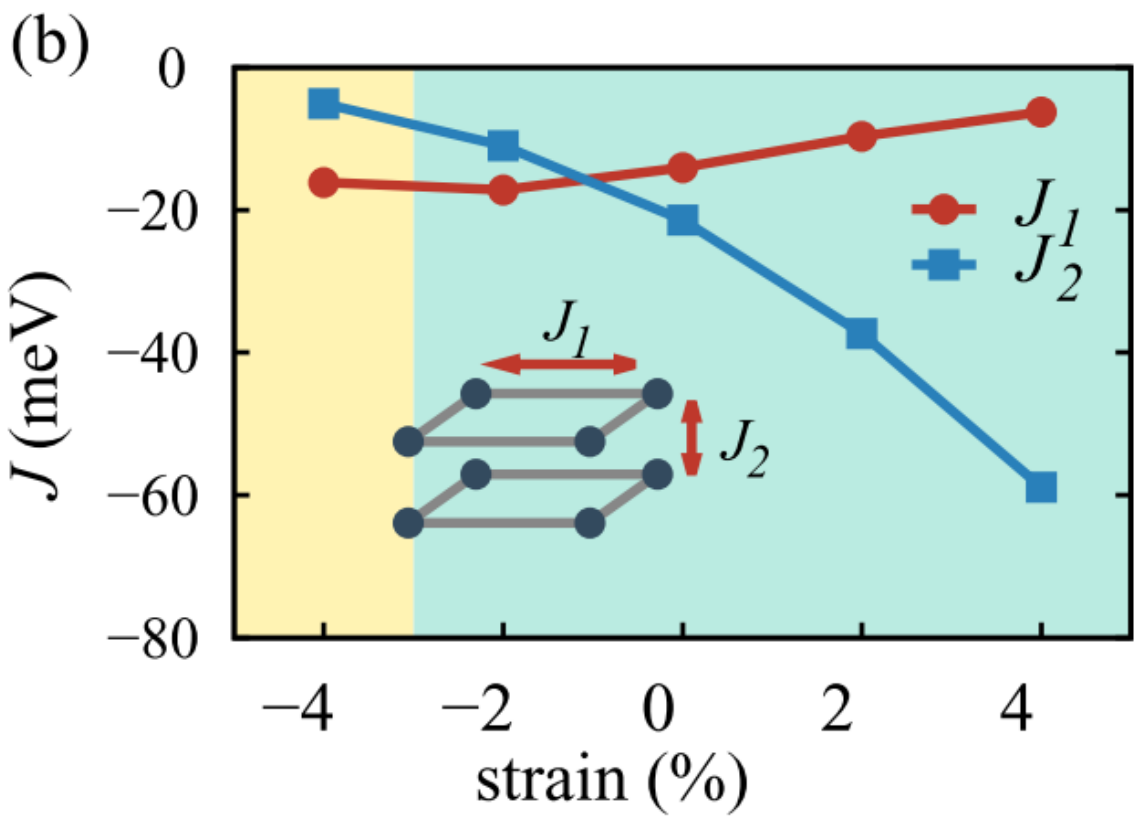

- Without epitaxial strain, $J_2 > J_1$, leading to out-of-plane magnetic order.
- Tensile strain favors out-of-plane magnetic order, whereas compressive strain induces spin-flip transition from out-of-plane spin to in-plane spin.

B. Kim, P. Liu and C. Franchini, 95, 024406 (2017)

Outline:

- Motivation
- Electronic properties
  - Combined effect of SOC and U
  - Doping induced MIT
- Magnetic properties
  - Origin of different magnetic orderings in Sr_2IrO_4 and $Sr_3Ir_2O_7$
- Optical properties
- Summary

Optical properties— GW+BSE

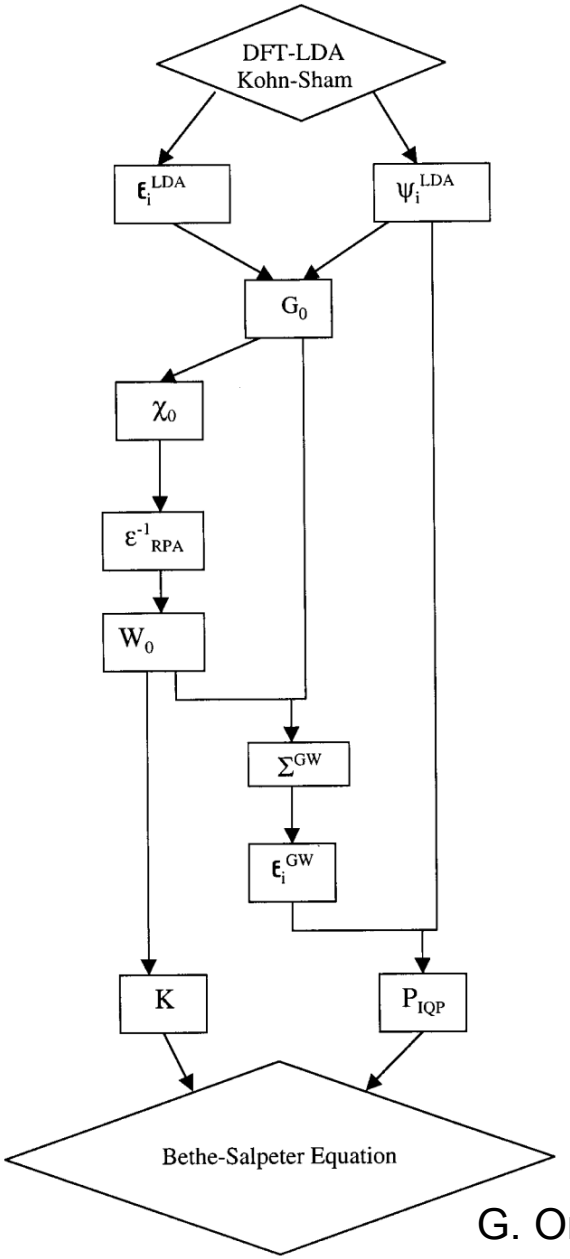

$$\chi^{-1}(\omega) = P^{-1}_{\mathrm{IQP}}(\omega) - K$$

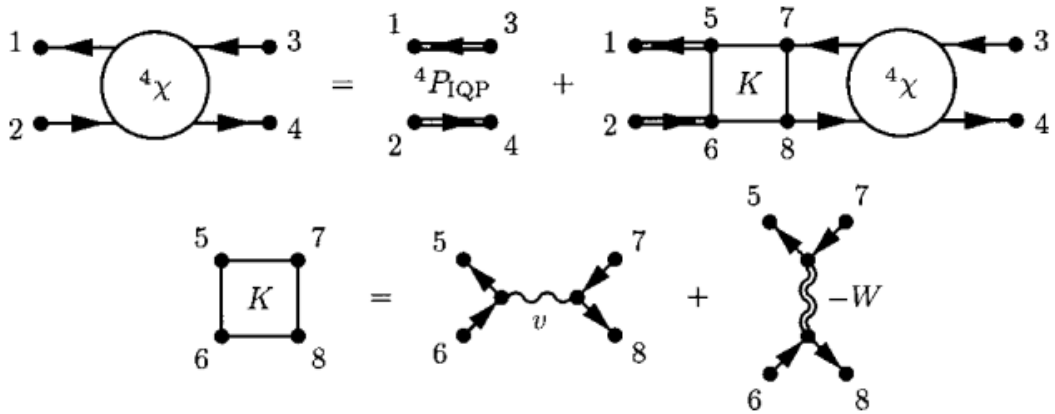

FIG. 3. Feynman diagrams representing the Bethe-Salpeter equation for χ.

G. Onida *et al.*, Rev. Mod. Phys. 74, 601 (2002)

Optical properties— GW+BSE

- Full BSE

$$\chi^{-1}(\omega) = P^{-1}_{\mathrm{IQP}}(\omega) - K$$

$$\begin{pmatrix} A & B \\ B & A \end{pmatrix}\begin{pmatrix} X_\lambda \\ Y_\lambda \end{pmatrix} = \Omega_\lambda \begin{pmatrix} \mathbf{1} & 0 \\ 0 & -\mathbf{1} \end{pmatrix}\begin{pmatrix} X_\lambda \\ Y_\lambda \end{pmatrix}$$

$$\begin{pmatrix} A & B \\ B & A \end{pmatrix} = \begin{pmatrix} K^{(\mathrm{r,r})} + (\varepsilon_a - \varepsilon_i)\delta^a{}_b\delta^i{}_j & K^{(\mathrm{r,a})} \\ K^{(\mathrm{r,a})} & K^{(\mathrm{r,r})} + (\varepsilon_a - \varepsilon_i)\delta^a{}_b\delta^i{}_j \end{pmatrix}$$

- Tamm-Dancoff approximation (TDA)

$$\begin{pmatrix} A & \cancel{B} \\ \cancel{B} & A \end{pmatrix}\begin{pmatrix} X_\lambda \\ Y_\lambda \end{pmatrix} = \Omega_\lambda \begin{pmatrix} \mathbf{1} & 0 \\ 0 & -\mathbf{1} \end{pmatrix}\begin{pmatrix} X_\lambda \\ Y_\lambda \end{pmatrix}$$

Optical properties— GW+BSE

➢ Tamm-Dancoff approximation (TDA)

- Frequency-dependent macroscopic dielectric function

$$\varepsilon(\omega) = 1 - \lim_{\mathbf{q}\to 0} V(\mathbf{q}) \sum_{\Lambda} \left(\frac{1}{\omega - \Omega_\Lambda + i\eta} - \frac{1}{\omega + \Omega_\Lambda - i\eta} \right)$$

$$\times \left\{ \sum_{\mathbf{k}} w_{\mathbf{k}} \sum_{v,c} \langle \psi_{c\mathbf{k}} | e^{i\mathbf{q}\cdot\mathbf{r}} | \psi_{v\mathbf{k}} \rangle X^{\Lambda}_{cv\mathbf{k}} \right\} \times \{\text{c.c.}\}, \qquad (4)$$

- Oscillator strength of optical transition

$$S_\Lambda = \mathbf{Tr}\left[\left\{ \sum_{\mathbf{k}} w_{\mathbf{k}} \sum_{v,c} \langle \psi_{c\mathbf{k}} | e^{i\mathbf{q}\cdot\mathbf{r}} | \psi_{v\mathbf{k}} \rangle X^{\Lambda}_{cv\mathbf{k}} \right\} \times \{\text{c.c.}\} \right]. \quad (5)$$

P. Liu *et al.,* PRM 2, 075003 (2018)

Optical properties— GW+BSE

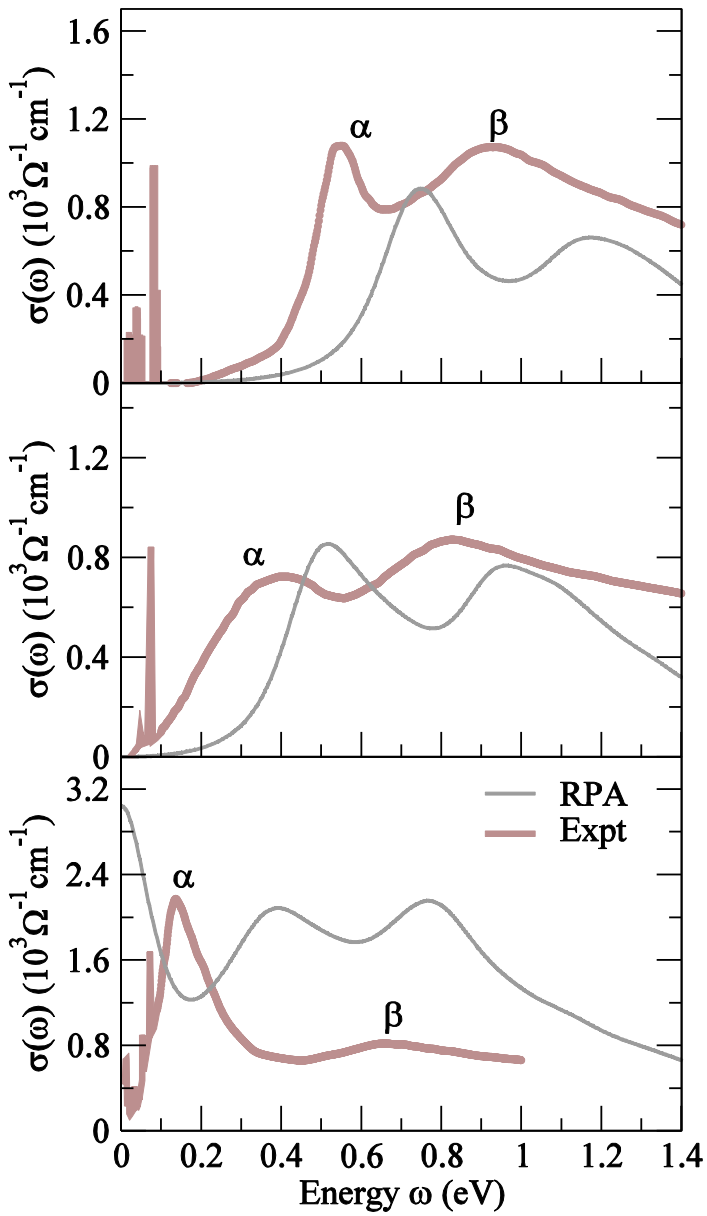

➢RPA

$$\chi^{-1}(\omega) = P^{-1}_{\mathrm{IQP}}(\omega) - K$$

$$K = V$$

$$\sigma_D(\omega) = \frac{\Gamma \omega_p^2}{4\pi(\omega^2 + \Gamma^2)}$$

P. Liu *et al.*, PRM 2, 075003 (2018)

Optical properties— GW+BSE

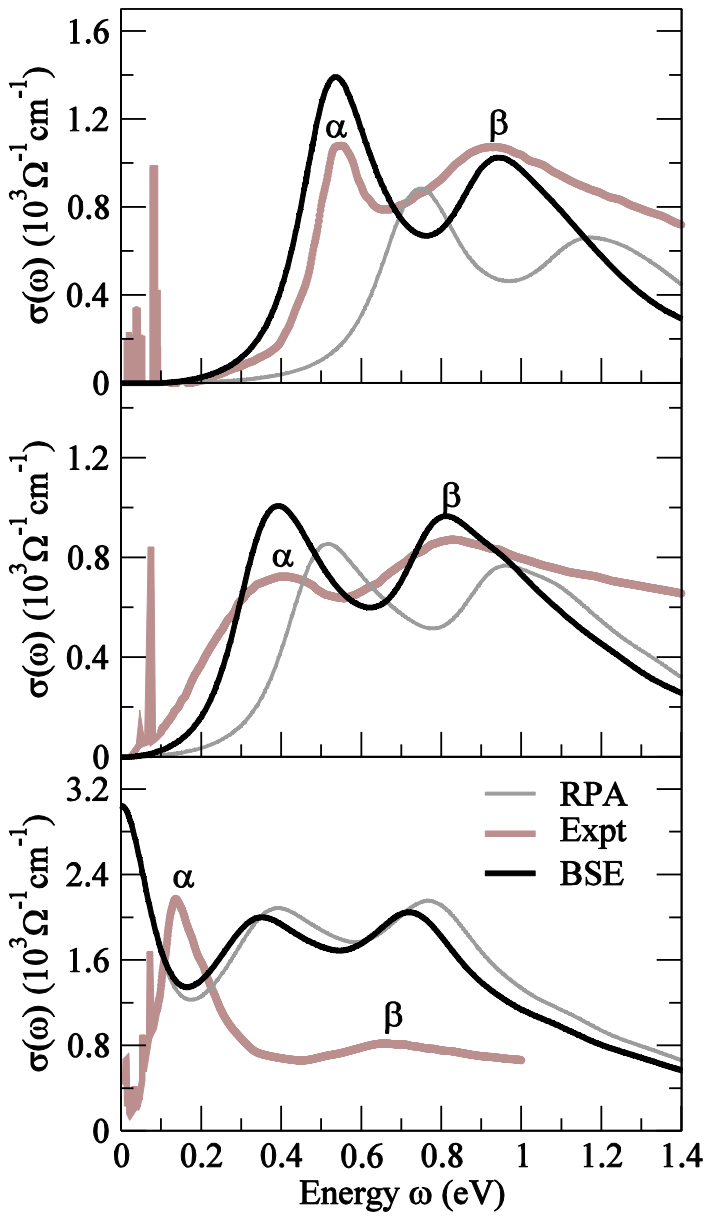

➢BSE

$$\chi^{-1}(\omega) = P^{-1}_{\mathrm{IQP}}(\omega) - K$$

$$K = V - W$$

P. Liu *et al.*, PRM 2, 075003 (2018)

Optical properties— GW+BSE

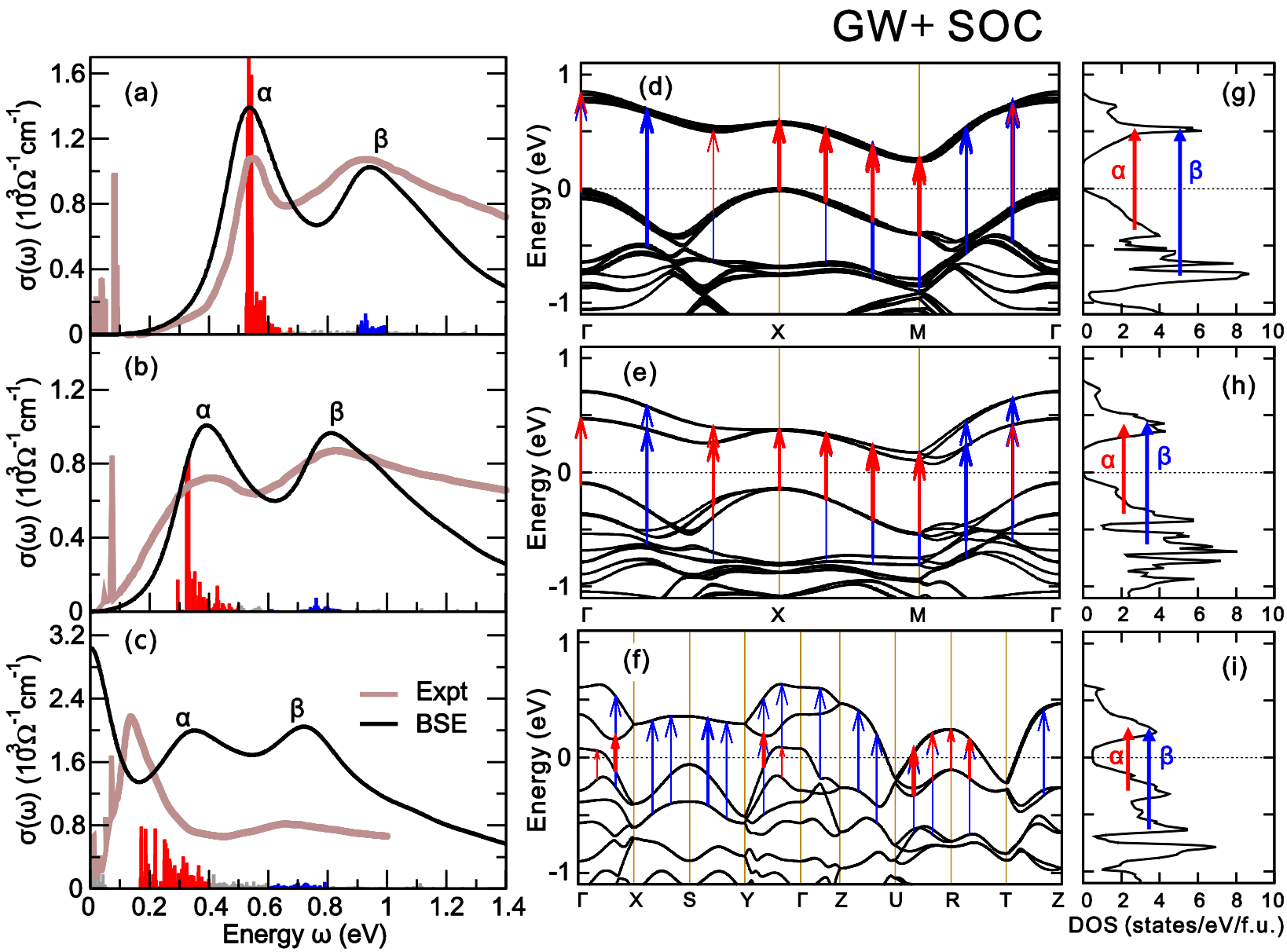

P. Liu *et al.*, PRM 2, 075003 (2018)

Optical properties— GW+BSE

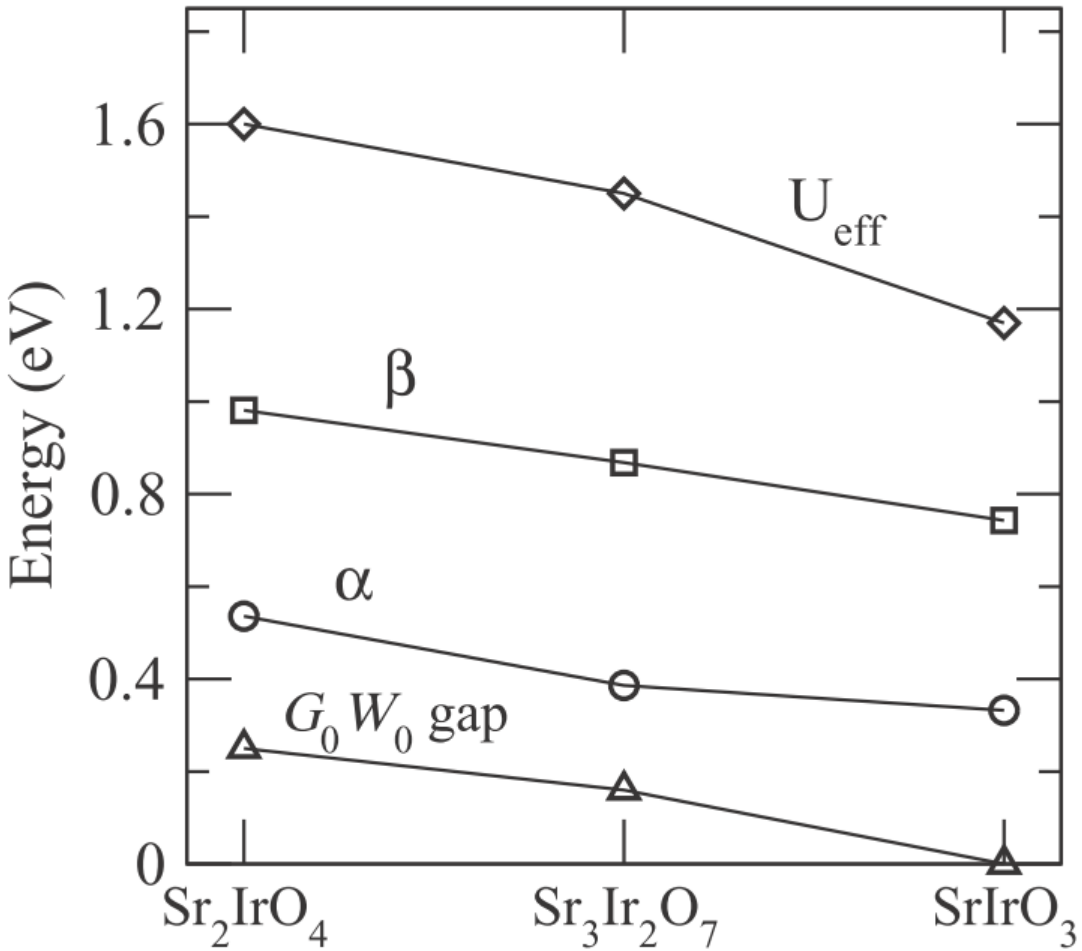

P. Liu *et al.,* PRM 2, 075003 (2018)

Summary

- The MIT phase diagrams w.r.t. SOC and U provide clear evidence for the relativistic Mott-Hubbard character in Sr_2IrO_4 and $Sr_3Ir_2O_7$.

- IMT is observed in La- and Rh- doped Sr2IrO4, which can be regarded as an effective electron and hole doping, respectively.

- The origin of the canted magnetic state in Sr_2IrO_4 arises from the competition between the isotropic exchange and DM interactions. The out-of-plane magnetic ordering of $Sr_3Ir_2O_7$ originates from strong interlayer exchange coupling.

- The GW+BSE optical spectra of Sr_2IrO_4 and $Sr_3Ir_2O_7$ agree well with the experimental results, but for $SrIrO_3$ the agreement is not good, though the double-peak feature is reproduced, indicating that going beyond GW is necessary to accurately describe the band renormalization for correlated metals.

Acknowledgment

Cesare Franchini

Univ. of Vienna

Bongjae Kim

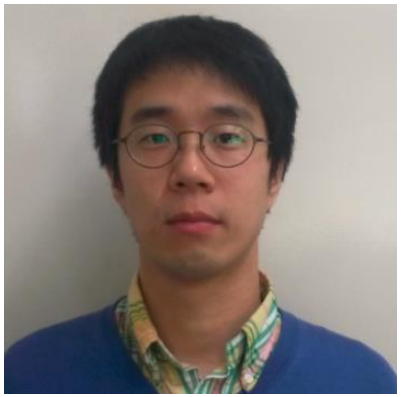

Kunsan National Univ.

Sergii Khmelevskyi

Univ. of Vienna

Georg Kresse

Univ. of Vienna

FWF

Der Wissenschaftsfonds.

VIENNA SCIENTIFIC CLUSTER

Thank you all for your attention!